

Fly palaeo-evo-devo: Immature stages of bibionomorphan dipterans in Baltic and Bitterfeld amber

Viktor A Baranov Corresp., 1, Mario Schädel 1, Joachim T Haug 1, 2

Corresponding Author: Viktor A Baranov

Email address: baranow@biologie.uni-muenchen.de

Larvae of flies and gnats (Diptera) form a crucial component of many terrestrial and freshwater ecosystems in the extant biosphere. Larvae of Diptera are playing a central role in water purification, matter and energy transfer in riparian ecosystems in rivers, carbon cycling in lakes and forests as well as being major decomposers of dead organic matter. Despite all these important roles, dipteran larvae are most often ignored in palaeoecological studies, due to the difficulty of the taxonomic identification of fossil larva, but also, due to the perceived importance of adult dipterans in palaeoentomological and taxonomic studies. Despite that, much information on palaeoecosystems can be gained from studying fossil dipteran larvae, in particular for well preserved specimens from fossil resins (ambers and copals). Since ambers are selectively preserving fauna of trunks and leaf litter, it allows us to learn a lot about xylophages and saprophages of amber forests, such as Eocene Baltic amber forest. Here we present immature stages (larvae and pupa) of the dipteran ingroup Bibionomorpha, from Baltic and Bitterfeld amber forests. We have recorded at least four different larval morphotypes, one with four distinct instars, and at least three pupal morphotypes. One larva is recognised as a new species and can be interpreted either as a representative of a highly derived ingroup of Bibionidae or as a sister species to Bibionidae. Also represented by single larval specimens are the groups Pachyneura (Pachyneuridae) and Sylvicola (Anisopodidae). The majority of the recorded specimens are representatives of the group Mycetobia (Anisopodidae). Due to the abundance of immature stages of Mycetobia, we have been able to reconstruct the number of larval stages (4) and relative growth rate of these fossil dipterans. We discuss implications of these finds.

 $^{^{}m 1}$ Biology II, Ludwig-Maximilians-Universität München, Planegg, Bayern, Германия

² Geobio-Center, Ludwig-Maximilians-Universität München, Planegg, Bayern, Германия



1	
2	Fly palaeo-evo-devo: Immature stages of
3	bibionomorphan dipterans in Baltic and Bitterfeld
4	amber
5	
6	
7	Viktor Baranov ¹ , Mario Schädel ¹ , Joachim T. Haug ^{1, 2}
8	¹ Biology II, Ludwig-Maximilians-Universität München, Planegg, Bayern, Germany
9	² Geobio-Center, Ludwig-Maximilians-Universität München, Planegg, Bayern, Germany
10	
11	Corresponding Author:
12	Viktor Baranov ¹
13	Biology II, Ludwig-Maximilians-Universität München, Planegg, Bayern, Germany
14	Email address: <u>baranow@biologie.uni-muenchen.de</u>
15	





Abstract

18 Larvae of flies and gnats (Diptera) form a crucial component of many terrestrial and freshwater 19 ecosystems in the extant biosphere. Larvae of Diptera are playing a central role in water 20 purification, matter and energy transfer in riparian ecosystems in rivers, carbon cycling in lakes and forests as well as being major decomposers of dead organic matter. Despite all these 21 important roles, dipteran larvae are most often ignored in palaeoecological studies, due to the 22 23 difficulty of the taxonomic identification of fossil larva, but also, due to the perceived importance of adult dipterans in palaeoentomological and taxonomic studies. Despite that, much 24 information on palaeoecosystems can be gained from studying fossil dipteran larvae, in 25 particular for well preserved specimens from fossil resins (ambers and copals). Since ambers are 26 selectively preserving fauna of trunks and leaf litter, it allows us to learn a lot about xylophages 27 28 and saprophages of amber forests, such as Eocene Baltic amber forest. Here we present immature 29 stages (larvae and pupa) of the dipteran ingroup Bibionomorpha, from Baltic and Bitterfeld 30 amber forests. We have recorded at least four different larval morphotypes, one with four distinct 31 instars, and at least three pupal morphotypes. One larva is recognised as a new species and can 32 be interpreted either as a representative of a highly derived ingroup of Bibionidae or as a sister 33 species to Bibionidae. Also represented by single larval specimens are the groups Pachyneura (Pachyneuridae) and Sylvicola (Anisopodidae). The majority of the recorded specimens are 34 representatives of the group Mycetobia (Anisopodidae). Due to the abundance of immature 35 36 stages of Mycetobia, we have been able to reconstruct the number of larval stages (4) and 37 relative growth rate of these fossil dipterans. We discuss implications of these finds.



Introduction

Holometabola is a hyperdiverse group of organisms, representing the dominant part of animal life in terrestrial ecosystems (Grimaldi & Engel, 2005). Representatives of the group such as bees, butterflies, beetles and mosquitoes are therefore the best known forms of Insecta to most people. The dominance of holometabloans has led researchers to consider Holometabola as one of the largest groups of Metazoa (Grimaldi & Engel, 2005, Engel, 2019). The evolution of niche differentiation between the larva and the adult (see Haug, in press) has been interpreted as one of the driving factors of their success. The evolutionary independence of different life stages and phases (see Scholtz, 2005) has allowed holometabolans to utilize a very wide spectrum of habitats and ecological niches (Grimaldi & Engel, 2005).

Larvae of flies and midges (representatives of the group Diptera) are successful in diverse habitats, from glaciers at the Antarctic mainland to the fast-drying rock pools of central Africa (Marshall, 2012; Armitage et al., 1995). Due to such variety of habitats occupied, larvae of Diptera have become involved in numerous critical ecosystem functions (Marshall, 2012). Dipteran larvae are crucial saprophages, recycling dead organic matter in both aquatic and terrestrial ecosystems, and therefore heavily influence biogeochemical cycles of matter and energy, for example in riparian ecosystems (Marshall, 2012; McAlister, 2017). This ecological role of larval forms of Diptera became especially important about 80 million years ago, in the Upper Cretaceous, when due to the Cretaceous Terrestrial Revolution (CTR) angiosperm plants have become the dominant players in the ecosystem (Fastovsky et al., 2004; Mckenna et al., 2015).

The emergence of angiosperm plants in terrestrial ecosystem probably led to an increased load of dead organic matter into terrestrial and freshwater ecosystems (Kalugina, 1974a, b; Mckenna et al., 2015). Such a drastic ecosystem change has led to shifts in the communities of various lineages of Insecta (Kalugina, 1974a, b). Such shifts included the extinction or decline of certain systematic and ecological groups. Among them were nectic and benthic oxyphilic forms living in dystrophic lakes. Vice versa, other groups, such as specialized pollinators or saprophages, have experienced an enormous diversification (Sinichenkova & Zherikhin, 1996). Among the groups experiencing a pronounced diversification were many ingroups of Diptera (Grimaldi & Engel, 2005). Numerous groups of dipterans with terrestrial larvae are associated with decaying organic material, such as dead wood, fungal fruit bodies, dead leaves, or animals corpses (Keilin & Tate, 1940; Marshall, 2012). Among the most abundant extant saprophagous forms of Diptera (with predominantly terrestrial larvae) are representatives of Bibionomorpha (Marshall, 2012; Ševčík et al., 2016).

Bibionomorpha includes numerous ingroups withecologically diverse representatives. However, larvae of Bibionomorpha are predominantly restricted to terrestrial habitats (Fig. 1, modified and simplified from Ševčík et al., 2016).

The geological history of Bibionomorpha spans more than 220 million years (Blagoderov et al., 2007). Many representatives are known from the late Triassic (Blagoderov et



al., 2007) and Jurassic (Kalugina and Kovalev, 1985). Despite the long evolutionary history of the group and the ecological importance of their larval stages, very little attention has been paid to the fossil record of immature stages of Bibionomorpha (Harris, 1983; Skartveit, 2008). This is surprising, as immature representatives of Bibionomorpha, especially those of Anisopodidae, seem to be quite common in amber, as we will demonstrate Despite such abundance, Anisopodidae larvae from amber were only mentioned in a single study focused on specimens from Dominican amber (Grimaldi, 1991).

Here, we present a first overview of the immature stages of Bibionomorphan from amber, including larvae and pupae of Anisopodidae, larvae of Pachyneuridae and a species that seems closely related to Bibionidae. All specimens in focus of this study are preserved in Eocene Bitterfeld amber and Baltic ambers (Table 1). We also discuss the implications of the morphological and ecological diversity of immature representatives of Bibionomorpha in relation to the ecology and biogeochemistry of the Eocene amber forests.

Materials & Methods

Material

All specimens in the center of this study, in total 56, are preserved in amber and come from various collections. A full list of the examined material is given in Table 1.

Part of the material (see table 1, material marked as "Material from Hoffeins collection") was obtained commercially in 2005 and stems from Yantarnyj, Kaliningrad district (formerly Palmnicken, Königsberg); specimens have temporarily been part of the collection of Christel and Hans-Werner Hoffeins (CCHH). All specimens from this source are now deposited at the Senckenberg Deutsches Entomologisches Institut (SDEI; with inventory numbers listed in table 1).

Another part of the material comes from the private collection of Carsten Gröhn and is now deposited in the collection of the Center for Natural History in Hamburg (Centrum für Naturkunde, CeNak, formerly Geological-Paleontological Institute and Museum of the University of Hamburg, Geologisch-Paläontologisches Institut und Museum der Universität Hamburg, GPIH).

Part of the material has been commercially obtained from Jonas Damzen ("amberinclusions.eu") by one of the authors. This material is now permanently housed in the research collection of the Palaeo-Evo-Devo Research Group, Ludwig-Maximilians-Universtät, Munich, Germany (PED). One specimen is part of the collection of the Museum für Naturkunde Berlin (MfNB).

Further material was retrieved from the collection of the Center for Natural History in Hamburg (CeNak).

Information on syninclusions is provided in table 1 as well. All abbreviations of the collection names are according to the "The insect and spider collections of the world" website (Evenhuis, 2019).



For comparative purposes, we used extant larval representatives of Anisopodidae and Bibionidae (larvae, pupae, and adult) from the collection of the Zoological State Collection, Munich (Zoologische Staatssammlung München, ZSM), in particular, *Sylvicola fenestralis* (Scopoli, 1763) (adult and pupa), *Mycetobia pallipes* Meigen, 1818 (larvae, pupae and adult, no collection number available) and *Penthetria funebris* Meigen, 1804 (larvae, pupae and adult, no collection number available) as well as *Bibio varipies* Meigen, 1830, (Centrum für Naturkunde Hamburg – CeNak, no collection number assigned).

The morphological terminology largely follows Borkent and Sinclair (2017). Yet, to enhance the understandability for non-experts, we amended some of the special morphological terms with more general terms. As Insecta is an accepted ingroup of Eucrustacea s.l. "crustacean"-terms are given in square brackets were necessary to provide wider frame correspondence.

Imaging methods

The specimens were imaged using a Keyence VHX-6000 Digital microscope, with ring-light type illumination and/or cross-polarised, co-axial illumination. All photographic images presented in this paper are composite images. Images were assembled using panoramic stitching to overcome the limitation of the field of view at higher magnifications. For each single image a stack of images of shifting focus was recorded to overcome the limitation of the depth of field (Haug et al. 2008, 2011, 2013a). Fusion into sharp images and panoramic stitching was performed with the software implemented in the digital microscope (e.g. Haug et al. 2018, 2019). We also used the implemented HDR function of the digital microscope; therefore every single frame is a composite from several images taken under different exposure times (cf. Haug et al. 2013b).

In addition to that, extant and fossil material was imaged using a Keyence BZ-9000 fluorescence microscope with either a 2x, 4x, 10x or 20x objective depending on the size of the objects. Observations were conducted at a emitted wavelength of 532 nm since it was the most compatible with the fluorescence capacities of the fossil specimens (Haug et al. 2011). To counteract the limitation in the depth of the focus we recorded stacks of images which than were digitally fused to single in-focus images using CombineZP (GNU). Extant specimens were imaged using a ZEISS Stemi 508 Stereo Microscope (with 8:1 Zoom with double LED spot K and additional ring light) in combination with a DCM 510 ocular camera and. Adobe Photoshop Elements 11 was used to stitch different images to single panoramic images. The resulting images were post-processed in Adobe Photoshop Elements 11 to optimize the histogram and sharpness as well as to amend the images with color markings to highlight morphological structures.

Two specimens (Dip-00653, Dip-00660) were scanned using X-Ray computer tomograph Zeiss Xradia XCT-200 in the Zoological Institute and Museum of University of Greifswald. Volume rendering images of the scans were created using Drishti (GNU) (e.g. Hörnig et al. 2016).



Micro-CT scanning of one specimen (MB.I.7295) was performed using a Nanotom m Phoenix (GE Sensing & Inspection Technologies GmbH). Scans were reconstructed to tiff stacks with the built-in software. Tiff stacks were further processed with ImageJ and Osirix 5.8.2 (e.g. Haug et al. 2011; Nagler et al. 2017).

Morphometry

Maximum head capsule length (in dorsal view) and width of some larvae were measured, as suggested by Coomb et al. (1997), from photos, using ImageJ (public domain; Schneider et al., 2012). Statistical analysis of the data was performed in R (GNU), using the mblm-function of the mblm-package, with a Theil-Sen single median method as a baseline method for applying Sen slopes to the data (Komsta, 2013). Not all specimens of the Mycetobia larvae had well preserved head capsule, therefore measurements of the width and length were performed for 25 specimens.

<u>Taxonomy</u>

Wherever possible we decided not to use Linnean ranks ("rankless taxonomy"). Ranks represent arbitrary constructs in a way that they do not hold "comparative values" (Mayr, 1942, p. 291, line 3) and, in our view, do not contribute to an easier understanding of phylogenetic relations among species and higher groups. However, the rank of the genus is not as easy to dismiss as the ranks of higher (broader) systematic groups. This is solely due to its function as part of binomial species names. Even though there are ways to avoid this dilemma such as the application of uninomial nomenclature for species (Lanham, 1965) or the use of any higher systematic group (regardless ranked as genus or not) as part of the species name (Haug & Haug 2016 following Béthoux 2010), the traditional, rank based, application of binomial names is still required by the International Code of Zoological Nomenclature (ICZN, Chapter 2, Article 5 & App. B, 6.). To be consistent with the "Code" we establish a new generic name, even though there is only one species assigned to this name and thus the sole purpose of this name is to serve as part of the binomial species name. Hence, until a sister taxon (species or group) to the herein described species is found, the generic name is that of a monotypic taxon and thus no diagnosis can be given for it.

For the sake of consistency, reproducibility and to increase the speed of fossil biodiversity discovery, we applied a matrix-based description scheme, proposed by Haug et al., (2012). We think that such form of description, based on the alternating characters states, entered in the excel sheet are useful in providing consistent, streamlined description, albeit with numerous repetitions of the same phrases.

A single new species is described herein. The electronic version of this article will represent a published work according to the International Commission on Zoological Nomenclature (ICZN), and hence the new names contained in the electronic version are effectively published according to the ICZN from the electronic edition alone. This published work and the nomenclatural acts it contains have been registered in ZooBank, the online registration system of the ICZN. The ZooBank LSIDs (Life Science Identifiers) can be resolved





and the associated information viewed through any standard web browser by appending the 197 LSID to the prefix http://zoobank.org/. The LSID for this publication is: 198 urn:lsid:zoobank.org:pub:7E6FFA31-9DA8-44A6-BE7D-55E6AE34B660. The online version of 199 this work is archived and available from the following digital repositories: PeerJ, PubMed 200 201 Central and CLOCKSS. 202 203 204 Results 205 206 **Taxonomy** Diptera Linnaeus, 1758 207 Bibonomorpha sensu lato sensu Ševčík et al., 2016 208 Dinobibio gen. nov. 209 Life Science Identifier: urn:lsid:zoobank.org:act:8C8DCD9A-1A44-473E-9692-210 211 54C7AE204B91. 212 Etymology: from Ancient Greek δεινός (deinos), meaning 'terrible, potent or fearfully great', due to the imposing nature of the larva, which bears large protuberances, and Bibio (ingroup of 213 214 Bibionidae). 215 Type species: Dinobibio hoffeinseorum sp. nov. by present designation. 216 Life Science Identifier: urn:lsid:zoobank.org:act:80D4F834-D0D4-404F-AE02-C8FF184D4943 217 218 *Remark*: no diagnosis can be given, since the new generic name does not refer to a natural group 219 but is only put up to provide a binomial name (see explanation above). However, for the 220 221 purposes of consistency we are providing putative diagnosis, identical, but abbreviated in comparison to the type species. Larva characterized by cylindrical body-shape; maxillary palp 222 223 with additional strong process distally on the element 1; trunk protuberances expanding towards 224 mid length and then tapering again; terminal abdominal spiracle, situated dorso-laterally, not larger than the rest of the spiracles. 225 226 227 228 Dinobibio hoffeinseorum sp. nov. 229 (Figs. 2A, 2B; 3A–D, Fig. S1) 230 231 Holotype: a single fossil larva, GPIH-0024 The larva is well preserved, but lateral aspects are 232 obscured by a silvery film (probably air bubbles) covering parts of the trunk. 233 234 Etymology: named after Christel and Hans-Werner Hoffeins for their immense contribution to 235 the general study of dipterans preserved in Baltic amber and Bibionidae in particular. 236

PeerJ

237 Syninclusions: a single "acalyptrate" fly ("Acalyptrata" = non-monophyletic assemblage of lineages within Brachycera that are not part of Calyptrata). Syninclusion too poorly preserved to 238 239 identify more precisely. 240 241 242 Description: 243 244 **Habitus**. Medium sized larva with a bowling-pin shaped body. Total length 6.4 mm. Body 245 differentiated into presumably 20 segments, ocular segment plus 19 post-ocular segments. 246 Head. Ocular segment and post-ocular segment 1–5 (presumably) forming distinct capsule (head 247 capsule). Head capsule longer than wide. Head capsule in dorsal view not accessible due to 248 orientation of the specimen. Hind part of head capsule partly retracted into anterior trunk. 249 Dimensions of head capsule: 860 um long, width hard to access. Surface of head capsule with 250 "warty" appearance, bearing numerous bulbous protrusions and smaller spine-like protrusions. 251 Ocular segment without apparent stemmata (larval eyes). Ocular segment recognizable by its 252 253 appendage derivative, clypeo-labral complex. Clypeus (clypear sclerite) dome-shaped, with several bulbous expansions on the top, total length 260 µm, oval in general shape (Figs. 3A, 3B). 254 Labrum not discernible. 255 **Post-ocular segment 1** recognizable by its appendages, antennae [antennulae]. Antenna arising 256 257 from head capsule postero-laterally to the clypeus. Antennae sitting on large piedestal (socket); no subdivision of antenna into elements apparent. (Figs. 3A-D) 258 Post-ocular segment 2 (intercalary segment) without externally recognizable structures. (Figs. 259 260 3A-D) **Post-ocular segment 3** recognizable by its pair of appendages, mandibles. Mandible only 261 262 accessible at the distal tip, proximal part obscured. (Figs. 3A-D) 263 **Post-ocular segment 4** recognizable by its appendage, maxilla [maxillula]. Maxilla massive, organised into proximal part and distal part, palp [endopod]. Proximal part differentiated into 264 two lobes, outer lobe and inner lobe. Inner lobe, possible lacinia [endite]. Possible lacinia 265 266 rectangular in outline. Possible lacinia 100 µm long, 200 µm wide. Palp arising from outer lobe, cylindrical, with two elements, palpomeres. Element 1 170 µm long. Element 1 distally with 267 strong conical outgrowth. Outgrowth 80 µm long. Element 2 conical, 45 µm long, without 268 269 apparent armature. (Figs. 3A-D) 270 Post-ocular segment 5 recognisable by its appendages, forming the labium [conjoined left and 271 right maxillae]. Labium massive, heavily sclerotized, with proximal part and distal parts, palps 272 [endopods]. Labium occupying over 60% of the total length of the head capsule ventrally. Palp 273 cylindrical, total length 35 μm (Figs. 3C, 3D). Total length of the labium (without palp) 310 μm, 274 width 200 µm. **Trunk.** Trunk roughly bowling-pin shaped, diameter increasing posteriorly along the trunk, 275 diameter of the trunk always larger than that of the head capsule (Figs. 2 A, B). Trunk with 12 276

visible units, interpreted as 3 thorax segments plus 8 abdominal units and a trunk end



- 278 representing a conjoined structure of undifferentiated abdominal segments (9–11?). Trunk with
- abdominal units, progressively increasing in lateral aspect towards the posterior part of the body.
- 280 Segment 1 1400 μm high, while 7th–1790 μm high. Trunk lacks parapodia and/or creeping
- 281 welts. Trunk bears dozens of conical protuberances on the entire surface. Each segment of the
- trunk, with the exception of the trunk end, carries 8 prominent, fleshy protuberances dorso-
- 283 laterally and ventrolaterally in groups of two, four at each side of the body. Protuberances widest
- at the mid-length, slightly narrower proximally part and tapering distally, mean length ca. 270
- 285 µm. Trunk surface with numerous small spines (Figs 2 A, B; Fig. S1). Trunk bears 10 pairs of
- spiracles (openings of the tracheal system) (Figs. 2, A,B). Each spiracle situated in the centre of
- an elevated ridge (Figs. 2 A, B).
- **Thorax** consists of three segments, pro-, meso- and metathorax.
- 289 **Prothorax** sub-equal in width to the head capsule, 670 µm. Prothorax bears a pair of large
- 290 spiracles. Prothorax carries 8 prominent, fleshy protuberances dorso-laterally and ventrolaterally
- in groups of two, four at each side of the body.
- 292 **Mesothorax** 580 µm long. Mesothorax carries 8 prominent, fleshy protuberances dorso-laterally
- and ventrolaterally in groups of two, four at each side of the body; Mesothorax with no spiracle
- 294 openings present.
- 295 Metathorax 560 µm long. Metathorax carries 8 prominent, fleshy protuberances dorso-laterally
- and ventrolaterally in groups of two, four at each side of the body. Metathorax bears a pair of
- 297 spiracles (Figs 2 A, B; Fig. S1).
- 298 Abdomen (posterior trunk) Height of abdominal units progressively increasing in lateral aspect
- 299 towards the posterior part of the body.
- 300 Abdominal units 1–8 each carrying 8 prominent fleshy protuberances dorso-laterally and
- 301 ventrolaterally in groups of two, four at each side of the body. Abdominal units 1–7 each
- 302 carrying a pair of spiracles laterally.

304 305

306

307

308

309 Abdominal unit 8 lacks spiracles.

- 310 **Trunk end** (undifferentiated abdomen segments 9–11?) shorter than abdominal unit 8. Trunk
- end bears anus on the posterior part. Trunk end bears more than a dozen of conical protuberances
- 312 on the entire surface. No protuberances present in the immediate vicinity of the anus, on the
- 313 postero-dorsal surface of the trunk end. Trunk end bears posterior spiracles with a single ecdysial
- 314 scar (a site where the previous larval stage cuticle breaks from the spiracle). Posterior spiracle is
- 315 sub-equal to the rest of the spiracles.

- 317 Differential diagnosis: The larva is clearly different from any modern representative of
- 318 Bibionidae, of which immature stages are known based on the combination of the following



characters: cylindrical body-shape; a maxillary palp with additional strong process distally on the element 1; trunk protuberances which are expanding towards mid length and then tapering again; terminal abdominal spiracle (abdominal segment 10), situated dorso-laterally, not larger then the rest of the spiracles; (Figs 2A, 2B; 3A–D).

Systematic interpretation, general body features: The general body shape, the absence of ambulatory legs on the thorax, as well as the spiracle arrangement is consistent with this larvae being an immature stage of the group Diptera. The larval specimen GPIH-0024 is interpreted to be clearly closely related to Bibionidae based on the following combination of characters (see Fig. 4A–C; 5 A–C): Head capsule fully sclerotized, posterior part of it is retracted into the prothorax; maxilla very short and stocky, with short and strong maxillary palp, head capsule black and shiny; eyes absent, antenna rudimentary; tracheal system holopneustic ("type 1" spiracles on the prothorax and metathorax, as well as on abdominal segments 1–7 & 9). Body heavily sclerotized, yet head capsule is sclerotized even more than the body. Prothorax is the longest segment of the trunk (Skartveit, 2017).

The very long and robust labium, the body with fleshy protuberances, bearing two rows of the protuberances dorsally and a single ecdysial scar on the posterior spiracle specimen, roughly resembles the condition in larvae of *Penthetria* Meigen, 1804 (Hennig, 1968, Skartveit, 2002), an ingroup of Bibionidae (Fig. 5A–C).

Systematic interpretation, head structures: The head capsule of the fossil larva is similar to that of larvae of Bibionidae. The antennae of the fossil larva are reduced as in larvae of Bibionidae. They are only represented by an undifferentiated conical piedestal in the fossil, similar to the condition in larvae of *Bibio* or *Penthetria* (both ingroups of Bibionidae; Fig. 5B, 5C). The maxilla of the fossil is robust, as it is in most larvae of Bibionidae. Yet, the larva differs in the structure of the maxillary palp (Fig. 4B, 4C): it is robust and cylindrical in general shape, similar to the representatives of *Penthetria* or *Bibio* (Figs. 4A–C, 5A–C), but differs drastically from the representatives of both groups by bearing a conical outgrowth distally on the first element of the palp (Figs 3A–D, 4A–C, 5A–C). This outgrowth is somewhat similar to the structure on the palpi of some extant larvae of Bibionidae. In particular, larvae of the ingroup of Bibionidae *Dilophus* possesses large, conical sensillae on the palpi. The outgrowth of the fossil larva is however much larger proportionally to the maxilla than that of larvae of *Dilophus*. Also it is situated on the distal part of the first element, not on the second element of the palp as it is the case for *Dilophus* (Krivosheina & Mamaev, 1967).

Other larval forms of Bibionomorpha that possess large sensilla on the maxillary palps are larvae of fungus-gnats Mycomyinae (Mycetophilidae; Krivosheina & Mamaev, 1967: figs. 31:1, 31:6). In contrast to larvae of Mycomyinae however, the outgrowths of the fossil larva are not articulated. We therefore argue that this is an unique character which is a putative autapomorphy of *Dinobibio hoffeinseorum* sp. nov..



The labium, in particular its proximal part, the mentum, is of the typical shape for larvae of Bibonidae (Figs. 3C, 3D), yet much broader and more robust than in any known larva of Bibionidae (s. 5A–C). The labium is occupying up to 60% of the entire width of the ventral area of the head, while the labium tin larvae of Bibionidae is much narrower, occupying about 20% of the ventral area of the head (Figs. 3 C, D, 5 B, C) (Skartveit, 2002). Mandibles and labrum are unavailable for a detailed examination due to being obscured by the other structures of the head.

Systematic interpretation, trunk structures: The general shape the body of the fossil larva is cylindrical with no parapods or other organs of locomotion (Fig 2A, 2B). Fleshy protuberances are protruding from the cuticle of the abdomen of the fossil larva. Numerous larvae of Bibionidae are exhibiting this condition as well. In particular, cuticular protuberances are typical for larvae of *Plecia* or *Penthetria* (both ingroups of Bibionidae) (Figs. 5A–C).

The protuberances of *D. hoffeinseorum* sp. nov. however differ from the protuberances of known larvae of Bibionidae, by their characteristic shape. The proximal attachment of the protuberances is relatively narrow expanding towards midlength, and narrowing towards conical distal end. (Figs. 2A, 2B). That character is differentiating *D. hoffeinseorum* sp. nov. from larvae of Bibionidae. In the latter the protuberances are simply tapering towards the tip (Fig. 2B). Additionally, the largest protuberances of *D. hoffeinseorum* sp. nov. are situated at the thorax and abdominal segments 1 and 2, in contrast to most larvae of Bibionidae, in which the length of the protuberances is increasing towards the posterior (Figs. 2A, 2B, Fig. S1). It is also possible, based on appearance, that the protuberances of *D. hoffeinseorum* sp. nov. are much more rigid than those of the known extant larvae of Bibionidae.

The tracheal system of the fossil larva is of the holopneustic type ("type 1",10 pairs of spiracles: one on the prothorax, one on the metathorax, one pair at abdominal units 1–7, and one pair at the trunk end; sensu Hennig, 1968). A holopneustic tracheal system is characteristic for larvae of Bibionidae.

The spiracle openings of the fossil larva are sitting on small elevated discs, representing a character state similar to that of some ingroups of Bibionidae. In larvae of Plecinae spiracle openings sit on conical outgrowths (Figs. 4A, 5B, 5C; cf. Skartveit, 2017). Most of the spiracles in the fossil are obscured by a silvery film, which, as it appears, formed by air, forced out from the tracheal system of the larva upon the entrapment in amber. Despite the obstruction of the view, the last tracheal spiracle pair (on abdominal unit 9) clearly has a single ecdysial scar, similar to larvae of *Penthetria* (Figs. 2A, 2B vs. 5A). In larvae of Bibionidae, the posterior spiraclesare positioned posterior-laterally on the trunk end (Skartveit, 2002, 2017; Skartveit and Willassen, 1996). In contrast to them, the posterior spiracles of the new larva are situated at the anterio-dorsal part of the trunk end. Also, the posterior spiracles of the new larva are not larger than the other spiracles of the same larva. This is in contrast to known larvae of Bibionidae.



In summary the fossil larva, here described as *D. hoffeinseorum* sp. nov. differs from any known larva of Bibionidae in three key characters: 1) a strong process at the distal end of element I of the maxilar palp, 2) a dorso-laterally position of spiracle 10. (on the trunk end); (Fig. S1); protuberances of unique shape.

Systematic interpretation, summary: In fact, the larva described as Dinobibio hoffeinseorum sp. nov. is so different from known larval forms of Bibionidae concerning the general body pattern and the arrangement of the spiracles in the tracheal system, that it cannot be easily interpreted as an ingroup of Bibionidae (Skartveit, 2008, 2017). We can think of two possible explanations for the distinctiveness of the D. hoffeinseorum sp. nov. in comparison to larvae of Bibionidae 1) D. hoffeinseorum sp. nov. is not an ingroup of Bibionidae, but rather a sister species to the group. 2) D. hoffeinseorum sp. nov. is representing a highly derived branch of Bibionidae, that is now extinct.

Neither of these explanations can be conclusively excluded, until further specimens of *D. hoffeinseorum* sp. nov. will become available, but it is beyond any doubt that this new species is very distinct from the rest of the known larvae of Bibionomorpha. The larvae of *D. hoffeinseorum* sp. nov. is exhibiting a curious mixture of traits, in this combination not known from any other larva of Diptera (cf. Kirk Spriggs and Sinclair, 2017). It does however possess the characters known from larvae of Bibionidae and Mycetophilidae, yet in an unusual combination (i.e. see the discussion of the maxilla palpi element one outgrowth).

In fact, such "impossible" character combinations, are quite common in the fossil record, representing an "experimental" phase of evolution, when a number of traits were independently evolving in different lineages (e.g. Haug et al., 2019). Theccurrence of such an unusual combination of characters might be a natural result of the "Push of the Past" effect, caused by the fact that most of the lineages surviving until the present, done so as a result of the initial diversification (Budd and Mann, 2018). On the other hand the unique combination of characters in *D. hoffeinseorum* sp. nov. might be indicative of the active diversification in Bibionomorpha in the Eocene, which challenges the common view of the representatives of Insecta in the Baltic amber fossils as being "mostly modern" (Zherikhin, 2003).

We would like to note that some colleagues have expressed reservations about describing new taxa based on immature stages. Yet, when it is possible to provide proper comparative diagnostics it is perfectly valid (according to ICZN) and also common to do this. In the present case the larva is so distinct that it is well possible to recognise the larva as a separate taxonomic entity.

Pachyneuridae + Hesperinidae (unnamed monophyletic group, Krivosheina, 2012)

- 434 Pachyneuridae Schiner, 1864
- 435 Pachyneura Zetterstedt, 1838
- 436 (Figs. 6A, 6B, 7A, 7B, 8A–D)



- 438 Material: A single fossil larva from the collection of Carsten Gröhn, which is now part of the
- 439 CeNak collection (Hamburg) with the collection number GPIH-L-7516. Specimen moderately
- well preserved, with posterior parts of the trunk obscured by cracks, lateral view not available. It
- appears that the specimen was desiccated before being encased in amber as evident from its
- somewhat distorted appearance.

444 Syninclusions: "Stellate hairs" (oak leaf trichomes).

- 446 Description:
- 447 Habitus. Medium sized larva with an dorso-ventrally flattened, spindle-shaped body. Total
- length 2.8 mm. Body differentiated into presumably 20 segments, ocular segment plus 19 post-
- ocular segments (Figs 6A, B, 7A, B).
- 450 **Head.** Ocular segment and post-ocular segment 1–5 (presumably) forming a distinct capsule
- 451 (head capsule). Head capsule wider than long. Hind part of head capsule not retracted into
- anterior trunk. Dimensions of head capsule: 450 µm long, 770 µm wide. Surface of head capsule
- smooth and glossy. Ocular segment without apparent stemmata (larval eyes) (9 A–D).
- 454 **Ocular segment** recognizable by its appendage derivative, clypeo-labral complex. Clypeus
- 455 (clypear sclerite) roughly rectangular, 200 μm long, 380 μm wide. Labrum small, weakly
- 456 sclerotized (Fig. 8C).
- 457 **Post-ocular segment 1** without externally recognizable structures. Antenna not discernible,
- 458 probably reduced. (Fig. 8A).
- 459 **Post-ocular segment 2** (intercalary segment) without externally recognizable structures (Fig.
- 460 8C).
- **Post-ocular segment 3** recognizable by its pair of appendages, mandibles. Mandible total length
- 462 220 μm, with 3 strong teeth on the apex, apical and subapical teeth sub-equal (all ca. 22 μm in
- length), molar tooth shorter (16 µm) (Fig. 8C).
- **Post-ocular segment 4** recognizable by its appendage, maxilla [maxillula]. Maxilla massive,
- organized into proximal part and distal part or palp [endopod]. Very proximal region with
- sclerite (hypostomal bridge). Further distal proximal part differentiated into two lobes, outer lobe
- and inner lobe. Inner lobe wth possible lacinia [endite]. Possible lacinia rectangular in outline,
- 468 100 μm long, 70 μm wide. Palp arising from outer lobe, cylindrical, with two elements
- 469 (palpomeres). Element 1 104 μm long, 45 μm long, with 4 hair-like setae distally (Fig. 8C).
- 470 **Post-ocular segment 5** recognizable by its appendages, forming the labium [conjoined left and
- 471 right maxillae]. Labium largely obscured by the large possible lacinia (Fig. 8C).
- 472 Trunk with 12 visible units, interpreted as 3 thorax segments plus 8 abdominal units and a trunk
- end, representing a conjoined structure of possibly undifferentiated abdominal segments (9–11?)
- 474 (Figs 6A, B; 7 A, B). Trunk widest at about half of the length with 910 µm, diameter decreasing
- posteriorly to 280 µm. Trunk with elevated ridges (possible creeping welts) at units 1-6 (three
- 476 thorax units, and first three units of the abdomen). Trunk surface with numerous small spines.
- 477 Trunk bears 10 pairs of spiracles (openings of the tracheal system). Spiracles surrounded by



- 478 lightly-coloured fields on the otherwise heavily sclerotized trunk units. Spiracles appear to have
- 479 single ecdysial scars.
- 480 Thorax consists of three segments, pro-, meso- and metathorax.
- **Prothorax** 80 μm long. Prothorax bears a pair of large spiracles. Prothorax subdivided into two
- 482 parts by annular constriction.
- 483 Mesothorax 95 µm long. No spiracle openings present. Mesothorax bears two lateral setae (ca.
- 484 70 µm long) on each side of the segment.
- 485 **Metathorax** 90 μm long. Metathorax bears two groups of dorsal setae (20–40 μm long), and two
- 486 lateral setae (ca 70 μm long) on each side of the segment. Metathorax bears a pair of spiracles.
- 487 **Abdomen (posterior trunk)** Abdominal units progressively increasing in dorsoventral aspect
- 488 towards the posterior part of the body, until reaching midlength of the abdomen, then decreasing
- 489 again, towards the trunk end.
- 490 Abdominal units 1–4, 6 bear two groups of dorsal setae (20-40 μm long), and two lateral setae
- 491 (ca 70 μm long) on each side of the segment. Units 1–8 each bearing a pair of spiracles laterally.

494

495 **Abdominal unit 5** (abdomen segment 5) bears two lateral setae (ca 70 μm long) on each side of the segment.

497

Abdominal unit 7 (abdomen segment 7) bears two lateral setae (ca $70~\mu m$ long) on each side of the segment.

499 500 501

498

Trunk end (undifferentiated abdomen segments 9–11?) obscured by cracks.

502

517

518

- 503 Systematic interpretation: The general body shape, as well as absence of ambulatory legs on the
- thorax, and the spiracle arrangement is consistent with this larva being an immature stage of
- Diptera. Numerous characters indicate that this is a larval form of Bibionomorpha: The larva
- possesses a very wide head capsule. The body as a whole is somewhat flattened dorso-ventrally,
- bearing six pairs of small ridges on the ventral side of the first six segments of the trunk (Figs.
- 508 6A, 6B, 7A, 7B).

The specimen is unusual by the combination of a holopneustic tracheal system ("type

- 510 2": spiracles (Hennig, 1968) on the prothorax, metathorax and abdominal segments 1–8, Fig 6B),
- presence of long setae on the abdomen, the head capsule being wider than long (Figs. 6A, 6B,
- 512 7A, 7B), prothorax being subdivided by a transversal furrow into the two rings (Figs. 6B, 7B).
- 513 All spiracles are surrounded by a lighter coloured area, in contrast to the more sclerotized parts
- of the segments. There are no other known larvae of Bibionomorpha with this state of characters.
- 515 It is possible however that the lighter areas are actually taphonomic artefacts, caused by air
- extrusions from the tracheal system upon the entrapment in amber.

The tracheal system with ten pairs of spiracles on the pro- and metathorax as well as on abdominal units 1–8 (Fig. 6B), is a synapomorphy of the bibionomorphan ingroups



Pachyneuridae + Hesperinidae (Krivosheina, 2012). The fossil is however distinct from larvae of Hesperinidae by bearing a large number of long setae (up to 70 μm long) on the abdominal units. Larvae of Hesperinidae possess only very short setae (Kivosheina, 2012). *Pachyneura* (only ingroup of Pachyneuridae sensu Paramonov and Salmela 2015) includes two species *Pachyneura fasciata* Zetterstedt, 1838 and *P. oculata* Krivosheina & Mamaev, 1972. Due to the suboptimal preservation of the larva, we decided not to formally describe a new species, as the resulting

526 527

528

529

530

531

532

533

525

In general, based on the combination of morphological characters, the larva appears to be a typical larva of *Pachyneura* (Pachyneuridae see Paramonov and Salmela 2015). This is the first and thus oldest fossil record of Pachyneuridae sensu Paramonov and Salmela (2015). Cramptonomyiidae, the sister group of Pachyneuridae+Hesperinidae, is present in the fossil record with representatives of its ingroups *Tega* Blagoderov, Krzeminska and Krzeminski, 1993 and *Pivus* Blagoderov, Krzeminska and Krzeminski, 1993 from Upper Jurassic respectively the Lower Cretaceous of Asia (Blagoderov et al., 1993).

534535

- 536 Anisopodidae Knab, 1912
- 537 Mycetobia Meigen, 1818

538

- 539 *Material:* 53 specimens of larvae and pupa in total were examined, see Table 1 for a complete
- list of the material. We were not able to distinguish distinct morphotypes for the larvae of
- 541 *Mycetobia*, while for the pupae three distinct morphotypes are apparent.

holotype would be not optimal for future comparative work.

542

- 543 Larvae
- 544 (Figs. 9 A–D; 10 A–E; Figs. S2–S10)

545

546 *Material:* see table 1 and Figs . 9 A–D; 10 A–E, Figs. S2–S10.

- 548 Description:
- Habitus. Medium sized larva with roughly vermiform body (9 A, B). Total length 1.8–10.2 mm
- 550 (all life stages; see table 2 for the summary of the morphometrics of the studied specimens) (10
- 551 A, B).
- Body differentiated into presumably 20 segments, ocular segment plus 19 post-ocular segments
- 553 (9 A-D, 10A-E).
- Head. Ocular segment and post-ocular segment 1–5 (presumably) forming distinct capsule (head
- capsule). Head capsule longer than wide. Head capsule well developed, fully sclerotized
- dorsally, partially sclerotized ventrally. Hind part of head capsule not retracted into anterior
- 557 trunk. Dimensions of head capsule: length 99–512 μm (n=25, all life stages), width 85–420 μm
- 558 (n=26, all life stages). Surface of head capsule smooth and glossy.



- Ocular segment without apparent stemmata (larval eyes). Ocular segment recognisable by its
- appendage derivative, clypeo-labrum complex (Figs 10 A, D).
- Post-ocular segment 1 recognizable by its appendages, antennae [antennulae]. Antenna
- represented by a single, cone-shaped element bearing a mushroom-like sensillum distally (Figs.
- 563 10 A, B, D, E).
- Post-ocular segment 2 (intercalary segment) without externally recognizable structures (Figs.
- 565 10 A, B).
- Post-ocular segment 3 recognizable by its pair of appendages, mandibles. Mandible divided into
- large, unsclerotized proximal portion, and heavily sclerotized distal portion, bearing numerous
- 568 teeth. (Figs. 10 A, B, D,E).
- Post-ocular segment 4 recognisable by its appendage, maxilla [maxillula]. Maxilla massive,
- organised into proximal part and distal part or palp [endopod]. Maxilla fleshy, very weakly
- 571 sclerotized, only general outline visible. Proximal part differentiated into two lobes, outer lobe
- and inner lobe. Palp small, stump-like (Figs. 10 A, B).
- Post-ocular segment 5 recognisable by its appendages, forming the labium [conjoined left and
- 574 right maxillae]. Labium, especially proximal part (mentum), narrow and weakly sclerotized,
- 575 trapezium-shaped. No distal structures (palpi) apparent. Posterior tentorial pits (external anchor
- point of the internal skeleton of the head capsule) present (Figs. 10 A, B).
- **Trunk.** Trunk composed of 11 visible units: pro-, meso- and metathorax, 7 abdominal units and
- 578 the trunk end. Trunk worm-like, units sub-equal in diameter (Figs. 9 A, B). Trunk lacks
- parapodia and/or creeping welts. Trunk bears two pars of spiracles: one on prothorax (Fig. 9 C)
- and one on trunk end (Figs. 9 C, D).
- **Thorax** consists of three segments, pro-, meso- and metathorax.
- **Prothorax** bears small, cone-shaped, anterior spiracles situated on posterolatero-dorsal surface.
- Prothorax subdivided into two unequal parts by annular constriction.
- Meso- and metathorax subequal to prothorax in length, but without annular constriction (Figs.
- 585 9 A, B).
- **Abdomen** (posterior trunk) with abdominal units cylindrical, roughly equal to each other in
- 587 diameter.
- **Abdominal units 1–7** subdivided into two unequal parts by annular constriction

591 592

593

- **Trunk end** (undifferentiated abdomen segments 8–11?) subdivided into three unequal parts by
- 597 two annular constrictions, with perianal shield (modified area of the last unit surrounding the
- anal aperture) on the ventral side. Trunk end bears posterior spiracles situated on the medio-



636

599 postero-dorsal surface of the unit. Spiracular field surrounded by 5 short lobes, bearing no apparent hairs (Figs. 9 A–D). 600 601 Systematic interpretation: 602 603 The general body shape, as well as the absence of ambulatory legs on the thorax, and the spiracle arrangement are consistent with these larvae being immature stages of the group Diptera. The 604 larvae furthermore show a distinct combination of characters: slender, vermiform body; head 605 sclerotized; dorsal part more strongly sclerotized than ventral one; mandible consists of fleshy 606 proximal part more heavily sclerotised distal part; prothorax and abdominal units 1–7 each 607 subdivided into two unequal parts by an annular constriction; respiratory system amphipmeustic; 608 anterior spiracles on a small cone on prothorax; posterior spiracles on spiracular field, on the 609 posterior of the trunk; trunk end covered by a perianal shield; the trunk end further subdivided 610 into three parts. 611 612 This character combination matches the condition in larvae of Anisopodidae (window gnats). Furthermore the fossil larvae show a spiracular disc surrounded by only very short lobes 613 and weak setae (Fig. 9 A–D, 11 A-D). This character is an autapomorphy of *Mycetobia* (ingroup 614 of Anisopodidae). 615 616 617 618 619 Pupae 620 621 Morphotype 1 (Fig. 12 A, B; Figs. S11–S26) 622 623 624 Material: see table 1 and Fig. 12 A, B; Figs. S11–S26 625 626 Description: 627 **Habitus.** Medium sized pupa, with generally comma-shaped body in lateral view (Figs. 12 A, B; Figs. S11–S26). Pupae coloured roughly in the same colour as the matrix of the amber. Total 628 629 length 2.7–5.1 mm long (n=14). See table 3 for a summary of the morphometrics. Body 630 differentiated into presumably 20 segments, ocular segment plus 19 post-ocular segments. Ocular segment and post-ocular segment 1–8 (presumably) forming a single globose unit (Figs. 631 632 12 A, B; Figs. S11–S26). 633 Ocular segment recognizable by its appendage derivative, clypeo-labrum complex and pair of large compound eyes. Labrum oval, slightly invaginated, membranous. Clypeus continuous with 634

labrum (Figs. 12 A, B, Figs. 21). Frons (frontal sclerite) with a pair of short setae, situated on top

of small conical warts. Setae of frontal sclerite longer than warts (Figs. 12 A, B; Fig. 21).

Peer| reviewing PDF | (2019:06:38366:1:1:NEW 29 |ul 2019)



- Post-ocular segment 1 recognizable by its appendages, antennae [antennulae]. Antenna
- 638 consisting of 16 elements. Antennae moderately long, following the dorso-posterior outlines of
- the compound eyes.
- Post-ocular segment 2 (intercalary segment) without externally recognizable structures (Figs.
- 641 12 A, B; Fig. S 21).
- Post-ocular segment 3 without externally recognizable structures (mandibles) (Figs. 12 A, B;
- 643 Sig. 21).
- Post-ocular segment 4 recognizable by its appendage, maxilla [maxillula]. Maxilla with
- proximal part (non-serrated "lacinia") and distal part, palp [endopod] (Figs. 12 A, B; Fig. S 21).
- Post-ocular segment 5 recognizable by its appendages, forming the labium [conjoined left and
- right maxillae]. Proximal parts of labium membranous, bears labial palps (Figs. 12 A, B; Fig. S
- 648 21).
- 649 Thorax consists of three segments, pro-, meso- and metathorax. Each bears a pair of
- 650 (ambulatory) appendages (fore-, mid- and hind legs). Wings on mesothorax; halterae on
- 651 metathorax. Thorax segments forming a single semiglobose structure, closely enveloping the
- 652 head (Figs. 12 A, B; Fig. S 21).
- 653 Ambulatory appendages (legs) U-shaped folded, running between the wings: mid- and hind
- legs terminating above the mid-length of the first posterior trunk (abdomen) unit. Ambulatory
- appendages curving between the wing tips, and then, diverging again after passing the tips of the
- wings (Figs. 12 A, B; Figs. S 21, 25, 26). All ambulatory appendages subdivided into the
- elements: coxa, trochanter, femur, tibia and tarsus (subdivided into 5 elements).
- Prothorax bears thoracic horns (modified spiracle 1). Thoracic horns club shaped, situated
- posterior to the eyes on the dorsal surface of the prothorax (Figs. 12 A, B). Prothorax bears 1st
- thoracic appendage pair (forelegs). Forelegs with femur and tibia forming a U-shaped loop, with
- anteriormost point of the loop reaching the level at which the maxillae arise.
- Mesothorax bears a pair of wings. Base of the wing aligned with the tip of the antennae.
- Midlegs underlying the forelegs, reaching beyond the tip of the wing.
- 664 **Metathorax** with a pair of spiracles. Hind legs underlying the forelegs and midlegs, reaching
- beyond the tip of the wing (Figs. 12 A, B).
- Length of head and thorax combined 1.0–2.3 mm (n=14). Abdomen 1.8–3.6 mm long (n=14).
- **Abdomen (posterior trunk).** With 9 units.
- **Abdominal units 1–8** each bearing two rings of strong hooklets. 12 hooklets in the first ring,
- 669 circa 70 hooklets in the second ring (Figs. 12 A, B). Abdominal units 2–8 each bearing a pair of
- 670 small spiracles (Figs. 12 A, B, Fig. S 21).

672

673

674

675 676

677



- **Trunk end** (undifferentiated abdomen segments 9–11?) bears a pair of the lateral expansions
- 680 (anal lobes) 8+2 hooklets. Hooklets arranged in 2 rings, two additional hooklets located on the
- anal lobes (Figs. 12 A, B; Fig. S 21). Abdomen length 1.7–3.6 mm (n=14).

- 683 *Mycetobia* pupa morphotype 2
- 684 (Figs. 13 A, B, Fig. S 27)

685

- 686 *Material:* This morphotype is represented by two pupae in our material; one specimen in the
- amber piece GPIH-7514 (originally from the collection of Carsten Gröhn), a second specimen in
- the amber piece PED-4866.

- 690 Description:
- 691 Habitus. Medium sized pupa, with generally comma-shaped body in lateral view. Pupa in
- 692 whitish-green to brown colours. Total length 4.3–5.3 mm long (n=2).
- Body differentiated into presumably 20 segments, ocular segment plus 19 post-ocular segments.
- Anterior part of the body composed of head and thorax, visible as a single globose structure
- 695 (Figs 13 A, B; Fig. S 27).
- 696 Ocular segment and post-ocular segment 1–5 (presumably) forming distinct capsule (head
- 697 capsule).
- 698 Ocular segment and post-ocular segment 1–5 (presumably) forming distinct caspule (head
- 699 capsule). Ocular segment recognizable by its appendage derivative, clypeo-labrum complex and
- 700 pair of large compound eyes. Labrum oval, slightly invaginated, membranous. Clypeus
- 701 continuous with labrum (Figs 13 A, B; Fig. S 27). Frons (frontal sclerite) of post-ocular segment
- 702 1 with a pair of short setae, situated on top of small conical warts. Setae of frontal sclerite shorter
- 703 than warts.
- 704 **Post-ocular segment 1** recognizable by its appendages, antennae [antennulae]. Antenna
- 705 consisting of 16 elements. (Figs 13 A, B; Fig. S 27). Antennae moderately long, following the
- 706 dorso-posterior outlines of the compound eyes.
- 707 **Post-ocular segment 2** (intercalary segment) without externally recognizable structures.
- 708 **Post-ocular segment 3** without externally recognizable structures (mandibles).
- 709 **Post-ocular segment 4** recognizable by its appendage, maxilla [maxillula]. Maxilla organised
- 710 into proximal part (non-serrated "lacinia") and distal part, palp [endopod].
- 711 **Post-ocular segment 5** recognizable by its appendages, forming the labium [conjoined left and
- 712 right maxillae]. Proximal part of labium membranous, bears labial palps (Figs 13 A, B; Fig. S
- 713 27).
- 714 Thorax consists of three segments, pro-, meso- and metathorax. Each bears a pairs of
- 715 (ambulatory) appendages (fore, mid-and hind legs). Wings on mesothorax. Halterae on
- 716 metathorax.
- 717 Thorax segments forming a single semiglobose structure, closely enveloping the head (Figs 13
- 718 A, B; Fig. S 27).



- 719 Ambulatory appendages (legs) U-shaped folded, running between the wings; mid- and hind
- 720 legs terminating anterior to the mid-length of the first posterior trunk (abdomen) unit.
- 721 Ambulatory appendages do not curve between the wing tips, width of the legs stays constant,
- 722 without divergence distally at the tips (Figs 13 A, B; Fig. S 27). All ambulatory appendages
- subdivided into the elements: coxa, trochanter, femur, tibia and tarsus (subdivided into 5
- 724 elements).
- 725 **Prothorax** bears thoracic horns (modified spiracle 1). Thoracic horns club shaped, situated
- posterior to the eyes on the dorsal surface. Forelegs superimposed over the thorax appendages 2
- and 3, not reaching wings tip. Forelegs with femur and tibia forming a U-shaped loop, with
- 728 anteriromost point of the loop reaching the level at which maxillae arise.
- 729 **Mesothorax** bears a pair of wing. Antennae do not reach the base of the wing. Midlegs
- 730 underlying the forelegs, reaching beyond the tip of the wing.
- 731 Metathorax bears a pair of halterae and a pair of spiracles. Hindlegs underlying the forelegs and
- midlegs, reaching beyond the tip of the wing (Figs 13 A, B; Fig. S 27).
- 733 Length of head and thorax combined 1.9–2.2 mm (n=2).
- 734 **Abdomen (posterior trunk).** With 9 units.
- Abdominal units 1–8 each bearing two rings of strong hooklets. Four hooklets in the first ring,
- 736 circa 48 hooklets in the second ring.
- 737
- 738 739
- 740
- 741
- 742743
- 1 +0
- **Trunk end** (undifferentiated abdomen segments 9–11?) bears 6 hooklets, two at the anal lobes
- 745 (Figs 13 A, B; Fig. S 27). Abdomen 2.7–3.2 mm long (n=2).
- 746 747
- **-** 40 3
- 748 *Mycetobia* pupa morphotype 3
- 749
- 750 (Figs. 14 A, B; Figs. S 28, 29)
- 751 *Material:* Morphotype 3 is represented by 2 specimens, one actual pupa and one adult emerging
- 752 from exuvium: table 1 and Figs. 14 A, B; Figs. S 28, 29.
- 753
- 754 Description:
- 755 **Habitus**. Medium-size insect pupae, with generally comma-shaped body. Pupae brown. Total
- 756 length 0.82–0.86 mm long (n=2). Body differentiated into presumably 20 segments, ocular
- respectively. Segment plus 19 post-ocular segments (Figs. 14 A, B; Figs. S 28, 29). Anterior part of the body
- 758 composed of head and thorax, visible as a single globose structure.



- 759 Ocular segment and post-ocular segment 1–5 (presumably) forming distinct capsule (head
- 760 capsule). Ocular segment and post-ocular segment 1–5 (presumably) forming a distinct capsule
- 761 (head capsule). Ocular segment recognisable by its appendage derivative, clypeo-labrum
- 762 complex and pair of large compound eyes. Labrum oval, slightly invaginated, membranous.
- 763 Clypeus continuous with labrum (Figs. 22 A–C). Frons (frontal sclerite) with a pair of short
- setae, situated on the top of small conical warts (Figs. 14 A, B; Figs. S 28, 29).
- **Post-ocular segment 1** recognisable by its appendages, antennae [antennulae]. Antenna
- 766 consisting of 16 elements. Antennae moderately long, following the dorso-posterior outlines of
- 767 the compound eyes.
- **Post-ocular segment 2** (intercalary segment) without externally recognisable structures.
- 769 **Post-ocular segment 3** without externally recognisable structures (mandibles) (Figs. 14 A, B;
- 770 Figs. S 28, 29).
- 771 **Post-ocular segment 4** recognisable by its appendage, maxilla [maxillula]. Maxilla with
- proximal part (non-serrated "lacinia") and distal part, palp [endopod] (Figs. 14 A, B; Figs. S 28,
- 773 29).
- 774 **Post-ocular segment 5** recognisable by its appendages, forming the labium [conjoined left and
- right maxillae]. Proximal part of labium membranous, bears labial palps (Figs. 14 A, B; Figs. S
- 776 28, 29).
- 777 Thorax consists of three segments, pro-, meso- and metathorax. Each bears a pairs of
- 778 (ambulatory) appendages (fore, mid-and hindlegs). Wings on mesothorax. Halterae on
- 779 metathorax.
- 780 Thorax segments forming a single semiglobose structure, closely enveloping the head of the
- 781 pupa.
- 782 Ambulatory appendages U-shaped folded, running between the wings; mid- and hind legs
- 783 terminating above the mid-length of the first posterior trunk (abdomen) unit. Ambulatory
- 784 appendages curving between the wing tips, and then, diverging again after passing the tips of the
- 785 wings (Figs. 14 A, B; Figs. S 28, 29). All ambulatory appendages subdivided into elements::
- 786 coxa, trochanter, femur, tibia and tarsus subdivided into 5 elements.
- 787 **Prothorax** bears thoracic horns (modified spiracle 1). Thoracic horns club shaped, situated
- 788 posterior to the eyes on the dorsal surface of the prothorax. Prothorax bears 1st thoracic
- appendage pair (forelegs). Forelegs superimposed over the thorax appendages 2 and 3, not
- reaching wings tip. Forelegs with femur and tibia forming a U-shaped loop, with anteriormost
- 791 point of the loop reaching the level at which maxillae arise (Figs. 14 A, B; Figs. S 28, 29).
- 792 **Mesothorax** bears a pair of wing. Midlegs underlying the forelegs, reaching beyond the tip of
- 793 the wing (Figs. 14 A, B; Figs. S 28, 29). Base of the wing aligned with the tip of the antennae.
- 794 **Metathorax** bears a pair of halterae and a pair of spiracles. Hindlegs underlying the forelegs
- and midlegs, reaching beyond the tip of the wing (Figs. 14 A, B; Figs. S 28, 29).. Base of the
- 796 wing aligned with the tip of the antennae.
- 797 **Abdomen (posterior trunk)** with 9 units. **Abdominal units 1-8** each bearing two rings of strong
- hooklets. 12 hooklets in the first ring, circa 70 hooklets in the second ring.



Trunk end (undifferentiated abdomen segments 9–11?) bears a pair of the lateral expansions (anal lobes) and 8+2 hooklets. Hooklets arranged in 2 rings, two additional hooklets sitting on anal lobes (Figs. 14 A, B; Figs. S 28, 29). Abdomen length 0.5–0.6 mm (n=2).

Systematic interpretation (all 3 morphotypes):

Pupae of all three morphotypes possess a single pair of wings on the mesothorax and developing halterae on the metathorax identifying them as pupae of the group Diptera. They are interpreted as representatives of Anisopodidae based on the following combination of characters: slender; antennae long, reaching, at least, until to the wing base; forelegs not reaching tip of wing, but mid and hindlegs reaching beyond the wings; thoracic horns small and oval to mushroom-like; spiracles present on metathorax and abdominal units 2–7. Last unit of abdomen bearing four pairs of strong denticles (Fig. 15 A–D).

Pupae of all three morphotypes possess characters autapomorphic for the group *Mycetobia* (ingroup of Anisopodidae): head bearing short frontal setae on conical warts; anterior and posterior margins of abdominal tergites bear rows of strong denticles.

Pupa morphotypes 1 and 2 can be distinguished from each other based on the number of denticles in the anterior row of the tergites, four in morphotype 2 and twelve in morphotype 1. Morphotype 1 can potentially include numerous species, indistinguishable in this stage and especially degree of preservation. Another diagnostic character differentiating the two morphotypes is the presence of a distal outward curvature of the legs of the morphotype 1, while morphotype 2 legs are of the constant width. Morphotype 3 is highly reminiscent of morphotype 1 but is significantly smaller, only about 30% of the total length of morphotype 1.

829 It

It is worth mentioning that the morphotypes might in fact result from sexual dimorphism. Yet, the examination of pupae of the extant species *Mycetobia pallipes* did not show any notable sexual dimorphism among the examined (non-pharrate) pupae, also not concerning size.

However, it will require examination of many more species of *Mycetobia* to draw any well-founded conclusions.

Taxonomic attribution: The morphology of both the larvae and the pupae is entirely in line with corresponding stages of extant representatives of *Mycetobia*. At least some of the representatives of pupa morphotype 1 are most likely representatives of *Mycetobia connexa*, which is the most abundant species of *Mycetobia* in Baltic amber (Wojton et al., 2019). This is indicated by the common preservation in the amber piece PED-4395, which contains a single exuvium of a pupa

of morphotype 1 as well as two adult representatives of Anisopodidae, a male and female (Figs.



841 S 11, 15). This male is a representative of *Mycetobia*, based on the following combination of characters: wing without discal cell, medial vein with three branches, radial vein 2+3 ending in 842 costa, radial vein 4+5 ending proximal to the end of the costal vein, anal vein 1 very faint 843 (Hancock, 2017). It can be interpreted as a representative of *Mycetobia connexa* Meunier, 1899 844 845 based on the following combination of characters: antenna elements (flagellomeres) 8–13 up to two times as long as wide; distal element of maxillary palp (palpomere) at most 3 times as long 846 as wide, thinned; subcostal vein ending proximal to radial sector bifurcation; radial vein 1 ending 847 on costal vein apex proximally of medial vein 1+2 bifurcation; fork of medial vein 1+2 wide; 848 medial vein 1+2 elongated, as long as medial vein 1; medial vein 2 and medial vein 3+4 849 separated by a distance at least two times as the distance between ends of the medial vein 1 and 850 medial vein 2; radial vein 2+3 two and 50% as long as radial sector or shorter; tarsus of foreleg 851 30% of the length of entire leg (including the coxa; Figs. S 11, 15) (Wojton et al., 2019a). We 852 interpret the male and the female of the *Mycetobia* inclusions in this piece as both being 853 854 representatives of *M. connexa* based on the identical wing venation and similar antennae. We have associated the pupal exuvium with the adults, based on their proximity in amber (Figs. S 855 856 11, 15). 857

It is so far impossible to determine associations of the studied larvae with any of the seven species of *Mycetobia* currently known from Eocene European ambers (Wojton et al., 2019). Future records of pupal exuvia with emerging or pharate adults and/or associated larval exuvia may allow for the association of further life stages. The record of three pupal morphotypes of *Mycetobia* in Baltic and Bitterfield amber is unsurprising, given the relatively high species richness of *Mycetobia* in those Lagerstätten (Wojton, et al., 2019).

862 863 864

858

859

860

861

865 Anisopodidae Knab, 1912

866 Sylvicola Fatio, 1867

867 (Figs. 16 A–D)

868

869 *Material*: Single larva, in Baltic amber, DEI Dip-00641.

870

871 Description:

Habitus. Medium sized larva with roughly vermiform body. Total length 6.4 mm. Body

873 differentiated into presumably 20 segments, ocular segment plus 19 post-ocular segments (Figs.

874 16 A–D).

875 **Head**. Ocular segment and post-ocular segment 1–5 (presumably) forming distinct caspule (head

876 capsule). Head capsule longer than wide. Head capsule well developed, fully sclerotized

877 dorsally, partially sclerotized ventrally. Head capsule in dorsal view not accessible due to

orientation of the specimen. Hind part of head capsule not retracted into anterior trunk. Head

879 capsule 280 μm long. Surface of head capsule smooth and glossy (Figs. 16 A–D).



- **Ocular segment** without apparent stemmata (larval eyes). Ocular segment recognisable by its
- appendage derivative, clypeo-labrum complex. Labrum 70 µm long (Figs. 16 A–D).
- 882 Post-ocular segment 1 recognizable by its appendages, antennae [antennulae]. Antenna conical,
- 883 consisting of one element, 44 µm long.
- Post-ocular segment 2 (intercalary segment) without externally recognizable structures.
- Post-ocular segment 3 recognisable by its pair of appendages, mandibles. Mandible only
- accessible at the distal tip, proximal part obscured. Mandible divided into large, unsclerotised
- proximal portion, and heavily sclerotized distal portion, bearing numerous teeth.
- **Post-ocular segment 4** recognisable by its appendage, maxilla [maxillula]. Maxilla massive,
- organised into proximal part and distal part, palp [endopod]. Proximal part of the maxilla fleshy,
- 890 very weakly sclerotized, only general outline visible. Maxilla bears six cone-like outgrows,
- probably sensillae. Proximal part differentiated into two lobes, outer lobe and inner lobe (Figs.
- 892 16 A–D).
- 893 **Post-ocular segment 5** recognisable by its appendages, forming the labium [conjoined left and
- 894 right maxillae].
- 895 Trunk composed of 11 visible units: pro-, meso- and metathorax plus 8 abdominal units. Trunk
- 896 worm-like, units sub-equal in diameter. Trunk lacks parapodia and/or creeping welts. Trunk
- bears two pars of spiracles, on prothorax and abdominal unit 8.
- 898 Thorax consists of three segments, pro-, meso- and metathorax.
- 899 **Prothorax** bears small, cone-shaped, anterior spiracles situated on postero-latero-dorsal surface.
- 900 Prothorax subdivided into two unequal parts by annular constriction.
- 901 Meso-and Metathorax subequal to prothorax, but without spiracles.
- 902 **Abdomen (posterior trunk)**. Abdominal units are cylindrical, roughly equal to each other in
- 903 diameter (Figs. 16 A–D).
- **Abdominal units 1–7** subdivided into two unequal parts by annular constriction.

907

908 909

910

911

912

- 913 **Trunk end** (undifferentiated abdomen segments 8–11?) subdivided into three unequal parts by two annular constrictions. Trunk end covered with perianal shield (modified area of the last unit
- 915 surrounding the anal aperture) on the ventral side. Trunk end bears posterior spiracles situated on
- 916 the medio-postero-dorsal surface of the unit. Spiracular field surrounded by five triangular,
- 917 setose lobes.

- 919 Systematic interpretation: The general body shape, as well as absence of the ambulatory legs on
- 920 the thorax, and the spiracle arrangement is consistent with this larva being an immature stage of



the group Diptera. Numerous characters indicate that the specimen is a larva of the group Anisopodidae: body slender, vermiform; head fully sclerotized, dorsal part more strongly sclerotized than ventral; mandible with fleshy proximal heavily sclerotized distal part; prothorax and abdominal segments 1–7 subdivided into the two unequal parts by an annular constriction; respiratory system amphipneustic; anterior spiracle forming small cone on prothorax; posterior spiracles on spiracular field, on the posterior end; trunk end with perianal shield; the trunk end subdivided into three parts.

The fossil larva possesses a spiracular disc surrounded by triangular setose lobes. The character is autapomorphic for the group *Sylvicola* (ingroup of Anisopodidae). In larvae of other ingroups of Anisopodidae the spiracle is surrounded by roundish lobes, bare of setae. The structure of the spiracular disc can be used to distinguish between larvae of *Mycetobia* and *Sylvicola* (Hanckock, 2017) also in fossilized resin.

The morphology of the fossil (Dip-00642) resembles extant larvae of *Sylvicola* to a high degree (cf. Keilin and Tate, 1940; Peterson,1981). Due to the preservation of the specimen, no characters could be observed to reliably differentiate between the fossil larva from larvae of the extant species *Sylvicola fenestralis* (Scopoli, 1763). It is also impossible to identify the larvae as a representative of any of the five known species of *Sylvicola* from Baltic amber, as all of them are known from adults only (Wojton, et al., 2018).

Syninclusions: stellate hairs and plant detritus are preserved in the same amber piece as the studied specimen.

Discussion

Species diversity and morphological diversity

Our investigations of Baltic and Bitterfeld amber material yielded at least four larval and three pupal morphotypes of Bibionomorpha. One larval type is even known from several instars.

There are probably numerous species of *Mycetobia* represented among the larval specimens. Yet, due to the degree of preservation it is impossible to distinguish them. The presence of several species within the material appears to be almost a certainty, taking into account the species diversity of Bibionomorpha in Baltic and Bitterfeld amber represented by adult forms, including at least 12 species of Anisopodidae (Wojton et al., 2018, 2019a, 2019b). Also, other bibionomorphan lineages show a quite rich fossil record in these amber Lagerstätten, again represented by adults, with at least 3 species of Hesperinidae, 10 species of Bibionidae and numerous species of the group Sciaroidea (Skartveit, 2002, 2008).

It is indeed surprising that the apparently abundant material of larvae and pupae of Bibionomorphan lineages in Eocene European amber has not attracted the attention of the scientific community earlier. There were some brief reports of pupae of Anisopodidae and Cecidomyiidae (Weitschat, 2009), but also these did not seem to attract much further attention. In a study by Haug et al. (2017), dealing with a group of dipteran pupae in a single amber piece, four specimens apparently representing morphotype 2 of *Mycetobia* have been reported (Haug et



al., 2017), yet misidentified as pupae of Asilidae, due to the somewhat similar structure of the spines or denticles on the trunk. Other pupae of Anisopodidae, without specification of further reaching taxonomic details have been reported from Miocene Dominican amber (Grimaldi, 1991).

No further immature stages of bibionomorphans have been reported from amber so far (Skartveit, 2017). This is probably a reflection of the fact, that in palaeoentomology, immature stages of the group Insecta often seem to be considered as 'inferior material' in comparison to adults. A possible reason for that is the relative difficulty of relating of taxa described based on larvae and pupae to the other taxa, which have been described based on adults. This might act as disincentive in a field, where α -taxonomy is still seen as a pinnacle of research achievement (Azar et al., 2018).

Still, taking in account the seeming general scarcity of larval forms of Diptera preserved in amber (Andersen et al., 2015, Baranov et al., 2019), the high abundance of larvae of Bibionomorpha in Eocene European ambers is remarkable. The taphonomic window of the fossilized resins seems strongly biased towards flying, hence adult representatives of Insecta (or better Pterygota), especially for adult forms of Diptera (Solórzano Kraemer et al., 2015). Larvae of Diptera often live in aquatic habitats, soil, leaf litter or are internal parasites of plants and animals and thus have limited opportunities for entrapment in plant resins and the subsequent preservation as amber inclusions (Solórzano Kraemeret al., 2015, Kirk-Spriggs, 2017).

Perkovsky et al. (2012) have shown that there is a stable structural cohort of animals preserved in Baltic and Rovno amber, which they termed "Sciara zone Diptera", which made up to 20% of all inclusion in representative batches of Baltic and Rovno amber. "Sciara-zone Diptera" is represented mostly by flies of the groups Bibionomorpha and Tipulomorpha, possessing xylophagous or saprophagous larvae, which apparently were associated with the tree-trunks in the Baltic amber forest (Perkovsky et al., 2012). Larval forms of "Sciara-zone Diptera", and especially those of Anisopodidae, are also living on tree trunks or right beneath them in the upper leaf-litter. This makes their preservation in fact highly likely in comparison to other larval forms of Diptera (Hancock, 2017). the preservation of a large number of immature of Mycetobia is in line with recent research on the entrapment bias in amber. This research (-Sánchez-García et al., 2017, Solórzano Kraemer et al., 2018) has shown that the taphonomic window of amber deposits is positively selecting towards fauna associated with tree trunks, while negatively selecting against species from the certain other habitats, i.e. hygropetric water films [aquatic habitats formed by the thin layers of water seepagin from the soil or bdroek] and true aquatic habitats (Sánchez-García et al., 2017).

Such a high abundance of larvae and pupae of Bibionomorpha provides an unprecedented look at the role of immature stages in the European Eocene amber forest. Since most of the immature stages of the Bibionomorpha in the studied material are closely reminiscent of corresponding stages of extant species, we can extrapolate the ecology of the fossil larval forms of Bibionomorpha to have been similar to their extant relatives (Seredszus and Wichard, 2008).



In fact, we have not been able to discern any substantial difference between studied larvae of *Mycetobia*, *Sylvicola* and *Pachyneura* preserved in amber and their extant counterparts. This is partially caused by the relatively low "resolution" of the characters in the fossil material, which does not allow to recognise more subtle differences between fossil larvae and their extant relatives.

Extant larvae of Pachyneuridae are associated with dead wood in pristine forests (Paramonov and Salmela, 2015). We assume a similar life habit for the fossil.

Extant larval representatives of *Mycetobia* and *Sylvicola* are associated with decaying organic material, mostly plant tissue. Yet, dung or animal corpses might also be occasionally exploited (Hancock, 2017). We can therefore assume that abundant larvae of *Mycetobia* (but also the larva of *Sylvicola*) preserved in Eocene amber were originally likewise connected to decaying organic matter. It is quite conceivable that a subtropical, seasonal forest in the Eocene of Europe would yield plenty of decaying organic matter, in the form of leaf litter, dead plant or animal matter, bacterial biofilms and fungi (Hancock, 2017, Wojton et al., 2019b).

Ontogeny of the fossil forms of Mycetobia

The relatively large amount of immature ("preimaginal") specimens of the species group ("genus") *Mycetobia*, allows to do a limited quantitative analysis of the post-embryonic ontogeny of these flies (Fig. 17). Coombs et al. (1997) have shown that representatives of Anisopodidae have four larval stages in their development. This was not based on rearing larvae in the lab, but rather on looking at the distribution of several morphometric parameters. Head capsule length, head capsule width and body length have been measured for 303 larvae of *Sylvicola fenestralis* (Scopoli, 1763). Coombs et al. (1997) found that at least the head capsule width distribution followed a distinct four-peak pattern, corresponding to four supposed larval stages for this species.

'Dyar's rule', describes the pattern of larval development in Holometobola (Dyar, 1890). In particular, it describes the inter-moult growth within Holometabola occurring at a similar rate for each larval stage. As a short remark: this pattern is even more general and not only true for Holometabola, but also for other crustaceans (cf. 'Brook's law', e.g. Fowler, 1909). This strict pattern can be used to infer the number of larval stages from the available dataset on larval morphometry (Coombs et al., 1997). In particular, mean values for every size cohort of log-transformed datasets should follow a straight line, with high values of R². If the mean values behave differently, deviating from a straight line, this would result in a larval stage (size cohort) missing from the plot (Dyar, 1890; Coombs et al., 1997). Coombs et al. (1997) have shown that the factor, with that the head capsule width increases between the larval stages of *Sylvicola fenestralis*, remains relatively constant (0.57–0.66) and follows Dyar's rule (Dyar, 1890; Coombs et al., 1997).

We applied the approach of Coombs et al. (1997) to our material and found that values plotted in increasing order; Figs. 18 A, 18 B) the head width and the head length of the fossil larvae of *Mycetobia* fall into four discrete categories (Figs. 19 A, 19 B). The line charted through



the ordered dot-plot has 3 clear breaks for both the head length and the width of the head, but not for the body length (Fig. 19). This indicates the presence of four larval stages (based on head capsule width). We think that the absence of such breaks in the body length plot, is connected to the taphonomic conditions of the larvae. It is possible that, upon the entrapment in amber, the larvae would shrink, obscuring the reconstruction of the original body length. In fact, McCoy et al. (2018) have shown by actuo-taphonomic experiments that the specific type of the fossil resin, desiccation prior to entombment and the composition of the gut microbiota all have a crucial impact on the preservation-quality of fossil insects. They have shown that the combination of the above mentioned factors will determine whether specimens will be preserved with soft tissue, as cuticular fossil only, or not at all (McCoy et al., 2019). Therefore, significant preservation biases can occur based on the identity of the insect and amber deposit. Therefore, it is even more advisable to use only hard sclerotized structures (such as head capsule), which are less prone to be deformed, for morphometrical purposes.

We proceeded to calculate the mean value of the head width and length for each of the cohorts observed in the plot. Then, those mean values were plotted against the supposed larval stage. Coombs et al. (1997) and Dyar (1890) have shown that if the values of morphometric parameters plotted against the supposed number of the larval stages are following a linear trend, that means that the studied sample contains all larval stages of the studied species (Fig. 17).

In our case, we have separated the stages based on the width of the head capsule, as Coombs et al. (1997) have shown it to be the most reliable predictor of the life-stage distribution in the measured larvae (Figs. 17, 18B). In our data the average values for both the head width and the head length follow a perfect linearly increasing trend-. The R² value for the head-width trend was 0.98 and 0.99 for the head length (Fig. 19).

Our data therefore supports the presence of four larval stages in the larval development of the Eocene *Mycetobia* species. The factor of growth between the stages is relatively steady, namely 0.6, and is consistent with Dyar's rule (Coombs et al., 1997; Table 2).

This is the first time that a full ontogenetic post-embryonic series of a dipteran could be reconstructed based on amber material. A more incomplete series of single larval stage, pupa and adult has been presented by Baranov et al. (2019). The reconstructed ontogeny of *Mycetobia* from amber demonstrates that during the Eocene Anisopodidae had lineages with representatives exhibiting derived morphologies and an ontogenetic development which is indistinguishable from extant forms of Anisopodidae (Wojton et al., 2019b).

Larvae of Bibionomorpha and amber forest ecology

Within the scientific community, a new understanding of the European Eocene amber forest (Schmidt et al., 2019, Seyfullah et al., 2018), as a warm-temperate seasonal forest, is currently emerging. This reconstruction is based on contemporary studies of palaeobotanical species complexes, fungi and microorganisms as well as isotope signatures, preserved in these ambers (Schmidt et al., 2019, Seyfullah et al., 2018). This reconstruction has currently not yet triggered



a re-interpretation of insect communities in these ambers, however it will likely cause such a reinterpretation in the future.

The major weakness of the current interpretation of the palaeoecology of Insecta in Eocene amber, is that it is based on a very coarse application of the uniformitarism principle to the ecology of now extinct groups (Grund, 2006; Seredszus and Wichard, 2011; Zelentsov et al., 2012; Baranov et al., 2015). This means there is a mechanistic phylogenetic inference, in which fossil representatives of species groups ("genera") are automatically assumed to have the autecological traits of the seemingly closest modern relatives. Yet, this is a mere oversimplification and likely malicious for the results and conclusions of such studies (Gründ, 2006). Many authors, have shown that in case of large and ecologically "diverse genera", or "relic genera" (groups which which were much more diverse in the past), such inferences might lead to the widely inaccurate conclusions (e.g. Stebner et al., 2018, Baranov et al., 2019a, b). This problem is of course also a result of the (unreflected) use of taxonomical ranks, as a low ranks (such as the genus) appear to suggest a close relationship among the included species. However, the assignment of ranks is a completely arbitrary decision (Mayr, 1942) and neither consistently reflects the age of a group nor the relatedness among species belonging to this group and as much less in a way that this would be comparable on a larger systematic scale (Dubois, 2007, Ereshefsky, 2002).

It is worth noting in this aspect, that the paleoecology of many fossil species with aquatic larvae such as non-biting midges (Diptera, Chironomidae) or caddisflies (Trichoptera) is interpreted based on the larval ecology of their extant relatives, yet inferred by fossils of the adults (for examples see Wichard et al., 2009). It is done in this way, as these groups of Insecta are widely used in aquatic biomonitoring today, and their larval habitats are thought to be rather narrow and well known (Merrit and Cummins, 1996).

The weakness of this approach for palaeohabitat reconstructions, is that it represents a type of double-inference, in case it is based on adults. 1) One infers a close relationship between the fossil (adult) animal and its extant relatives, for whichthe larval ecology is known. 2) One assumes that the larvae of the fossil adult animal behaved similar to their extant counterparts, without access to the larval morphology (Wichard et al., 2009).

A more direct interpretation of the ecology of larvae, which are more tied to particular habitats (in many lineages of Insecta larvae perform most of the ecological functions) is considered advantageous in comparison to the above mentioned double-inference. Such an advantage arises from the direct observation of the larval morphology, which in combination with the interpretation of the taphonomic situation and the possible presence of syninclusions can tell a lot about the ecology of an animal (Andersen et al., 2015; Baranov et al., 2019b).

Hence the observed details of immature forms of Bibionomorpha eliminate one level of assumptions and provide more direct indications of the palaeohabitat. The high abundance of immatures of Anisopodidae in Eocene European amber forests, may indicate moist conditions and a large amount of decaying organic matter on the forest floor, a habitat characteristic for extant representatives of Anisopodidae (Hancock, 2017). This is reaffirming similar conclusions



1120 made based on the abundant co-occurence of non-biting midges (Diptera, Chironomidae) with terrestrial larvae in Baltic amber (Andersen et al., 2015; Baranov et al., 2019). Secondly, the 1121 presence of a larva of Pachyneuridae (xylobiont-xylophages, living in the deep layer of xylem of 1122 1123 old, still living trees) is indicative for pristine temperate forests in extant conditions 1124 (Krivosheina, 2006; Paramonov and Salmela, 2016). Therefore, in the Eocene it might translate to mature forest communities with large quantities of the dead wood. Hence, the findings of 1125 larval forms of Diptera provide a new independent source of information that can be used for 1126 1127 palaeohabitat reconstruction.

11281129

11301131

1132

1133

11341135

1136

1137

1138

11391140

1141

11421143

1144

11451146

1147

1148

1149

Conclusions

This first examination of immatures of Bibionomorpha from Baltic and Bitterfeld amber is based on more than 60 specimens, representing three major ingroups of Bibionomorpha: Bibionidae (or a possible sister species to it), Pachyneuridae and Anisopodidae. Bibionidae (or its sister species) and Pachyneuridae are both represented by a single larval morphotype; Anisopodidae is represented by at least two larval morphotypes and at least three pupal morphotypes.

The larva of Pachyneura is the first fossil record for this group. The presence of this larva, indicates pristine, temperate forest conditions, with abundant old trees. This lines up well with the emerging new interpretation of the Baltic amber forest as a warm-temperate, seasonal ecosystem (Schmidt et al., 2019).

Window gnats (Diptera, Anisopodidae), are the most abundant immature stages of bibionomorphans in Bitterfeld and Baltic amber. A large number of fossil immatures allowed us to reconstruct the full post-embryonic ontogenetic series of fossil representatives of *Mycetobia* (Anisopodidae). This reconstruction is only the second one for dipterans in amber (first in Baranov et al., 2019b), and also the most complete. It demonstrates that in the Eocene representatives of *Mycetobia*, just as their extant counterparts, had four larval stages.

This study shows the large potential of future studies on fossil larvae of flies in amber. Contrary to the widespread opinion, these larvae are relatively abundant. Their abundance, and ecological information associated with them (plus the additional information from syninclusions and other clues about the taphonomy), might be crucial to further elucidate the new, emerging picture of the palaeoecosystems that are preserved by Baltic and Bitterfeld amber.

115011511152

1153

Acknowledgements

- VB is grateful to M. Spies and D. Doczkal (ZSM Munich) for his invaluable help with collection of ZSM as well as help with the literature. VB is grateful to M. K. Hörnig
- 1156 (University of Greifswald) for conducting MicroCt scanning of the Anisopodidae pupa. VB, MS
- and JTH are grateful to C. & H.-W. Hoffeins (Hamburg), C. Gröhn (Hamburg) and U. Kotthoff
- 1158 (CeNak, Hamburg) for providing access to the material. We are grateful to the editor and three



1159 1160 1161	anonymous reviewers for their efforts in improving this manuscript. Thanks to all people providing free software.
1162	
1163	
1164	
1165	Deference
1166	References
1167	Andersen T, Baranov V, Goral T, Langton P, Perkovsky E, Sykes D. 2015. First record of a
1168 1169	Chironomidae pupa in amber. Geobios 48(4): 281–286.
1170	Armitage PD, Pinder LC, Cranston, P. S. (Eds.). 2012. The Chironomidae: biology and ecology
1171	of non-biting midges. Springer Science & Business Media, London.
1172	
1173	Baranov V, Andersen T, Perkovsky, EE. 2015. Orthoclads from Eocene Amber from Sakhalin
1174 1175	(Diptera: Chironomidae, Orthocladiinae). Insect Systematics & Evolution 46(4): 359–378.
1176	Baranov V, Giłka W, Zakrzewska M, Jarzembowski E. 2019a. New non-biting midges (Diptera:
1177	Chironomidae) from Lower Cretaceous Wealden amber of the Isle of Wight (UK). Cretaceous
1178	Research 95: 138–145.
1179	
1180	Baranov V, Hoffeins C, Hoffeins, H-W, Haug JT. 2019b. More than dead males: reconstructing
1181	the ontogenetic series of terrestrial non-biting midges from the Eocene amber forest. Bulletin of
1182	Geosciences 94(2): 1-13.
1183 1184	Béthoux, O. 2010. Optimality of phylogenetic nomenclatural procedures. Organisms Diversity &
1185	Evolution 10: 173–191 DOI: 10.1007/s13127-010-0005-3.
1186	2701ddoi 10. 173 171 201. 10.1007/813127 010 0002 3.
1187	Blagoderov VA, Krzeminska E, Krzeminski W. 1993. Fossil and recent Anisopodomorpha
1188	(Diptera, Oligoneura): family Cramptonomyiidae. Acta zoologica cracoviensia, 35(3): 573–579.
1189	
1190	Blagoderov V, Grimaldi DA, Fraser NC. 2007. How time flies for flies: diverse Diptera from the
1191 1192	Triassic of Virginia and early radiation of the order. American Museum Novitates 3572: 1–39.
1193	Borkent A., Sinclair BJ. 2017. Key to Diptera families-larvae. In: Kirk-Spriggs AH, Sinclair B J.
1194	(Eds.). Manual of Afrotropical Diptera. Volume 1: Introductory chapters and keys to Diptera
1195	families. Suricata 4. South African National Biodiversity Institute, Pretoria; pp. 357–405.
1196	



- Budd, G. E., and Mann, R. P., 2018, History is written by the victors: The effect of the push of
- the past on the fossil record: Evolution, v. 72, no. 11, p. 2276-2291.

- 1200 Coombs RM, Cleworth MA, Davies DH. 1997. Determination of instar for the window gnat
- 1201 Sylvicola Fenestralis (Diptera: Anisopodidae). Water Research 31: 186–193.

1202

- 1203 Dubois, A. 2007. Phylogeny, taxonomy and nomenclature: the problem of taxonomic categories
- 1204 and of nomenclatural ranks. Zootaxa, 1519(1): 27– 8.

1205

- 1206 Dyar HG. 1890. The number of molts of lepidopterous larvae. Psyche: A Journal of Entomology
- 1207 5(175–176): 420–422.

1208

- 1209 Engel, M. 2019. Natural Histories. Innumerable insects. The stories of the most diverse and
- 1210 myriad animals on Earth. Sterling, New York.

1211

- 1212 Ereshefsky, M. 2002. Linnaean ranks: Vestiges of a bygone era. Philosophy of Science, 69(S3):
- 1213 S305–S315.

1214

- 1215 Evenhuis, N.L. 2019. The insect and spider collections of the world website. Available at:
- 1216 http://hbs.bishopmuseum.org/codens/ [Last accessed: 07.05.2019].

1217

- 1218 Fastovsky DE, Huang Y, Hsu J, Martin-McNaughton J, Sheehan PM, Weishampel DB. 2004.
- 1219 Shape of Mesozoic dinosaur richness. Geology 32: 877–880. https://doi.org/10.1130/G20695.1.

1220

- Fowler, G. H. 1909. Biscayan plankton collected during a cruise of H.M.S. 'Research' 1900. Part
- 1222 xii. The Ostracoda. Transactions of the Linnean Society of London (2), Zoology, x, pp. 219-336,
- 1223 12 pls.

1224

- 1225 Grimaldi DA. 1991. Mycetobiine woodgnats (Diptera, Anisopodidae) from the Oligo-Miocene
- amber of the Dominican Republic, and Old World affinities. American Museum novitates 3014:
- 1227 1–24.

1228

1229 Grimaldi D, Engel MS. 2005. Evolution of the Insects. Cambridge University Press.

1230

- 1231 Grund M. 2006. Chironomidae (Diptera) in Dominican amber as indicators for ecosystem
- stability in the Caribbean. Palaeogeography, Palaeoclimatology, Palaeoecology 241(3–4): 410–
- 1233 416.

- 1235 Harris AC. 1983. An Eocene larval insect fossil (Diptera: Bibionidae) from North Otago, New
- 1236 Zealand. Journal of the Royal Society of New Zealand 13(3): 93–105.



- 1237
- 1238 Haug, C., Mayer, G., Kutschera, V., Waloszek, D., Maas, A. & Haug, J. T. 2011. Imaging and
- documenting gammarideans. International Journal of Zoology, art. 380829, DOI
- 1240 10.1155/2011/380829.

- Haug, J. T., Briggs, D. E., & Haug, C. 2012. Morphology and function in the Cambrian Burgess
- 1243 Shale megacheiran arthropod Leanchoilia superlata and the application of a descriptive matrix.
- 1244 BMC Evolutionary Biology, 12(1), 162, https://doi.org/10.1186/1471-2148-12-162.

1245

- Haug, C., Shannon, K. R., Nyborg, T. & Vega, F. J. 2013b. Isolated mantis shrimp dactyli from
- the Pliocene of North Carolina and their bearing on the history of Stomatopoda. Bolétin de la
- 1248 Sociedad Geológica Mexicana 65, 273–284.

1249

- Haug, C., Herrera-Flórez, A. F., Müller, P. & Haug, J. T. 2019. Cretaceous chimera-an unusual
- 1251 100-million-year old neuropteran larva from the "experimental phase" of insect evolution.
- 1252 Palaeodiversity 12, 1–11.

1253

- Haug, J. T., Haug, C. and Ehrlich, M. 2008. First fossil stomatopod larva (Arthropoda:
- 1255 Crustacea) and a new way of documenting Solnhofen fossils (Upper Jurassic, Southern
- 1256 Germany). Palaeodiversity, 1: 103–109.

1257

- Haug, J. T., Haug, C., Kutschera, V., Mayer, G., Maas, A., Liebau, S., Castellani, C., Wolfram,
- 1259 U., Clarkson, E. N. K. and Waloszek, D. 2011. Autofluorescence imaging, an excellent tool for
- 1260 comparative morphology. Journal of Microscopy, 244: 259–272.

1261

- Haug, J. T., Müller, C. H. G. and Sombke, A. 2013a. A centipede nymph in Baltic amber and a
- new approach to document amber fossils. Organisms Diversity and Evolution, 13: 425–432.

1264

- Haug, J. T. & Haug, C. 2016. "Intermetamorphic" developmental stages in 150 million-year-old
- achelatan lobsters The case of the species tenera Oppel, 1862. Arthropod Structure &
- 1267 Development 45: 108–121 DOI: 10.1016/j.asd.2015.10.001.

1268

- Haug J. T. in press. Why the term "larva" is ambiguous, or what makes a larva? Acta Zoologica
- 1270 early view: 1–22.

1271

- Haug, J. T., Müller, P. & Haug, C. 2018. The ride of the parasite: a 100-million-year old mantis
- 1273 lacewing larva captured while mounting its spider host. Zoological Letters 4, 31.

1274

1275 Hancock EG. 2017. Anisopodidae (Wood Gnats or Window Gnats). In: Kirk-Spriggs, AH,



- 1276 Sinclair BJ. (Eds.). Manual of Afrotropical Diptera. Volume 2: Nematocerous Diptera and lower 1277 Brachycera. Suricata 5. South African National Biodiversity Institute, Pretoria; pp. 633–640. 1278 1279 Hennig W.1968 Die Larvenformen Der Diptera. Teil 1. Akademie-Verlag. Berlin. 1280 Hörnig, M. K., Sombke, A., Haug, C., Harzsch, S. & Haug, J. T. 2016. What nymphal 1281 morphology can tell us about parental investment – a group of cockroach hatchlings in Baltic 1282 Amber documented by a multi-method approach. Palaeontologia Electronica 19(1), art. 5A, 20 1283 1284 pp. 1285 1286 International Commission on Zoological Nomenclature. 2012. Available at http://www.nhm.ac.uk/hosted-sites/iczn/code/ (accessed 2 May 2019). 1287 1288 1289 Kalugina NS. 1974a. Eutrophication as one possible cause for the changes in aquatic biocenoses towards the end of the Mesozoic, pp. 137-139. In: Antropogennoe evtrofirovanie vod 1290 1291 [Anthropogenically eutrophied waters], Akademia Nauk SSSR, Chernogolov. 1292 1293 Kalugina NS. 1974b. Change in the subfamily composition of chironomids (Diptera, 1294 Chironomidae) as an indicator of possible eutrophication of bodies of water during the late 1295 Mesozoic. Journal of the Moscow Naturalist's Society 79: 45–56. 1296 1297 Kalugina NS, Kovalev VG. 1985. Jurassic Diptera of Siberia. Izdatelstvo Nauka, Moscow, 197 1298 pp. 1299 1300 Knab F. 1912. New species of Anisopodidae (Rhyphidae) from Tropical America. [Diptera: Nemocera.]. Proceedings of the Biological Society of Washington 25:111–114. 1301 1302 1303 Komsta L. 2013. mblm: median-based linear models. R package version 0.12. 1304 1305 Krivosheina NP. 2006. Taxonomic composition of dendrobiontic Diptera and the main trends of 1306 their adaptive radiation. Zoologicheskii Zhurnal 85 (7): 842–852. [in Russian] 1307 1308 Krivosheina M. 2012. Key to the families and genera of the Palearctic Dipterous insects of the suborder Nematocera, based on larvae [in Russian], Moscow, KMK Scientific press, 244 pp.+. 1309 1310
- 1311 Krivosheina NP, Mamaev BM. 1967. A Key to Dipteran Larvae Inhabiting Wood [In
- 1312 Russian]. Nauka Scientific Press, 266 pp.

- 1314 Krivosheina NP, Mamaev BM. 1972. New data on relict Diptera of the Pachyneuridae family.
- 1315 Nauchnye Doklady vysshey shkoly. Biological sciences 11: 13–18. [in Russian].



1316	
1317	Lanham, U. 1965. Uninominal nomenclature. Systematic Zoology 14: 144-144.
1318	
1319	Mayr, E. 1942. Systematics and the origin of species. New York: Columbia University Press.
1320	
1321	Marshall SA. 2012. Flies. The natural history and diversity of Diptera. Firefly Press Ltd, 616 pp.
1322	
1323	Meigen JW. 1804. Klassifikazion und Beschreibung der europäischen zweiflügligen Insekten.
1324	(Diptera Linn.). Erster Band, erste Abtheilung, mit VIII Kupfertafeln pp. I–XXVIII [= 1–28],
1325	1–152, Tab. I–VIII [= 1–8]. Braunschweig. (Reichard).
1326	
1327	Meigen JW. 1818. Systematische Beschreibung der bekannten europäischen zweiflügeligen
1328	Insekten. Erster Theil mit elf Kupfertafeln pp. I–XXXVI [= 1–36], 1–324, [1]. Aachen.
1329	(Forstmann).
1330	M '' DW C ' WW (E1) 1000 A ' 4 1 4' 4 41 4' ' ' 4 CN 41
1331	Merritt RW, Cummins KW. (Eds.). 1996. An introduction to the aquatic insects of North America. Kendall Hunt.
13321333	America. Kendan Hunt.
1334	Mckenna DD, Wild AL, Kanda K, Bellamy CL, Beutel RG, Caterino MS, Farnum CW, Hawks
1335	DC, Ivie MA, Jameson ML, Leschen LAB, Marvaldi AE, McHugh JV, Newton AF, Robertson
1336	JA, Thayer MK, Whiting MF, Lawrance JF, Slipinski A, Maddison DR, Farrel, BD. 2015. The
1337	beetle tree of life reveals that Coleoptera survived end-Permian mass extinction to diversify
1338	during the Cretaceous terrestrial revolution. Systematic Entomology 40(4): 835–880.
1339	https://doi.org/10.1111/syen.12132
1340	
1341	Nagler, C., Hyžný, M. & Haug, J. T. 2017. 168 million years old "marine lice" and the evolution
1342	of parasitism within isopods. BMC Evolutionary Biology 17, 76.
1343	
1344	Perkovsky EE, Rasnitsyn AP, Vlaskin AP, Rasnitsyn SP. 2012. Contribution to the study of the
1345	structure of amber forest communities based on analysis of syninclusions in the Rovno Amber
1346	(Late Eocene of Ukraine). Paleontological Journal 46(3): 293–301.
1347	
1348	Ponomarenko, AG. 2003. Ecological evolution of beetles (Insecta: Coleoptera). Acta zoologica
1349	cracoviensia 46.Suppl (2003): 319-328.
1350	
1351	Sánchez-García, A., Nel, A., Arillo, A., and Kraemer, M. M. S., 2017, The semi-aquatic
1352	pondweed bugs of a Cretaceous swamp: PeerJ, v. 5, p. e3760.
1353	
1354	Schneider CA; Rasband WS, Eliceiri KW. 2012. "NIH Image to ImageJ: 25 years of image
1355	analysis". Nature methods 9(7): 671–675.



1356	
1357	Schiner IR. 1864. Fauna Austriaca. Diptera. Vol. II. Wien : C. Gerolds Sohn, 1862-64.
1358	
1359	Schmidt AR., Sadowski E-M, Kunzmann L, Kaasalainen U, Seyfullah LJ, Rikkinen J. 2019.
1360	Reconstruction of amber forests using plants, lichens and fungi: a case study of the 'Baltic amber
1361	forest'. Abstracts of th 8th International Conference on Fossil insects, Arthropods and Amber.
1362	Santo-Domingo, 2019, 12–13
1363	
1364	Scholtz, G. (2005) Homology and ontogeny: Pattern and process in comparative developmental
1365	biology. Theory in Biosciences124:121-143.
1366	
1367	Scopoli JA. 1763. Entomologia Carniolica exhibens insecta Carnioliæ indigena et distributa in
1368	ordines, genera, species, varietates. Methodo Linnæana. pp. 1–420, [1]. Vindobonae. (Trattner).
1369	
1370	Seredszus F, Wichard W. 2011. Overview and descriptions of fossil non-biting midges in Baltic
1371	amber (Diptera: Chironomidae). Studia dipterologica 17: 121–129.
1372	¥ ¥ ¥
1373	Ševčík J, Kaspřák D, Mantič M, Fitzgerald S, Ševčíková T, Tóthová A, Jaschhof M. 2016.
1374	Molecular phylogeny of the megadiverse insect infraorder Bibionomorpha sensu lato
1375	(Diptera). PeerJ: 4, e2563.
1376	Confullability Deignfords C. Del Consert Demishat W. Dillain on J. Calonida A.D. 2010. Decidentics
1377	Seyfullah LJ, Beimforde C, Dal Corso J, Perrichot V, Rikkinen J, Schmidt AR. 2018. Production
1378	and preservation of resins – past and present. Biological Reviews 93(3): 1684–1714.
1379 1380	Skartveit J. 2002. The larvae of European Bibioninae (Diptera, Bibionidae). Journal of Natural
1381	History 36(4): 449–485.
1382	Thistory 30(4). 449–463.
1383	Skartveit J. 2009. Fossil Hesperinidae and Bibionidae from Baltic amber (Diptera:
1384	Bibionoidea). Studia dipterologica 15: 3–42.
1385	Diolonoldea). Studia dipterologica 15. 5 42.
1386	Skartveit J. 2017. Bibionidae (March flies or Lovebugs). In: Kirk-Spriggs AH, Sinclair, BJ.
1387	(Eds.). Manual of Afrotropical Diptera. Volume 2: Nematocerous Diptera and lower Brachycera.
1388	Suricata 5. South African National Biodiversity Institute, Pretoria, pp. 497–504.
1389	2022-000-00-00-00-00-00-00-00-00-00-00-0
1390	Skartveit J., Willassen E. 1996. Phylogenetic relationships in Bibioninae (Diptera, Bibionidae).
1391	Skarteveit, J. Studies on the systematics and life histories of Bibioninae (Diptera, Bibionidae). D.
1392	Phil. Thesis. University of Bergen, Bergen, Norway.
1393	





1394 1395	Solórzano-Kraemer MM, . Kraemer AS., Stebner F, Bickel DJ, Rust J. 2015. Entrapment bias of arthropods in Miocene amber revealed by trapping experiments in a tropical forest in Chiapas,
1396	Mexico. PloSOne 10(3): e0118820.
1397 1398	
1399	Solórzano Kraemer, M. M., Delclòs, X., Clapham, M. E., Arillo, A., Peris, D., Jäger, P., Stebner,
1400	F., and Peñalver, E., 2018, Arthropods in modern resins reveal if amber accurately recorded
1401	forest arthropod communities: Proceedings of the National Academy of Sciences, v. 115, no. 26,
1402	p. 6739-6744.
1403	
1404	Stebner F, Baranov V, Zakrzewska M, Singh H, Giłka W. 2017. The Chironomidae diversity
1405	based on records from early Eocene Cambay amber, India, with implications on habitats of fossil
1406	Diptera. Palaeogeography, Palaeoclimatology, Palaeoecology 475: 154–161.
1407	
1408	Wichard W, Gröhn C, Seredszus F. 2009. Aquatic insects in Baltic amber - Wasserinsekten im
1409 1410	Baltischen Bernstein. Verlag Kessel, Remagen-Oberwinter. [in English and German].
1411	Zelentsov NI., Baranov VA, Perkovsky EE, Shobanov NA. 2012. First records on non-biting
1412	midges (Diptera: Chironomidae) from the Rovno amber. Russian Entomological Journal 21: 79–
1413	87.
1414	
1415	Zetterstedt JW. 1838. Sectio tertia. Diptera. Dipterologis Scandinaviae amicis et popularibus
1416	carissimus. Insecta Lapponica. Lipsiae [=Leipzig], 392 pp.
1417	
1418	
1419	
1420	





PeerJ

1422	
1423	List of figures
1424	
1425	Figure 1. Phylogenetic relationship among different lineages of Bibionomorpha sensu lato,
1426	modified and simplified from Sevcik et al., 2016.
1427	
1428	Figure 2. Dipteran larva, holotype of <i>Dinobibio hoffeinseorum</i> sp. nov. GPIH, accession number
1429	(GPIH-0024) in lateral view. (A) overview, composite image. (B) coloured version of A above.
1430	Abbreviations: a1–a8, abdominal segment 1–8; hc, head capsule; mp, maxillary process; ms,
1431	mesothorax; mt, metathorax, pt, prothorax; s1-s10, spiracle 1–10; te, trunk end.
1432	
1433	Figure 3. Fossil dipteran larva, holotype of <i>Dinobibio hoffeinseorum</i> sp. nov. GPIH, accession
1434	number (GPIH-0024). (A) head capsule, latero-dorsal view; (B) coloured version of A. (C) head
1435 1436	capsule, ventrolateral view. (D) coloured version of C. Abbreviations: an, antennae; cl, clypeus;
1437	he, head capsule; lb, labium; md, mandible; mp, maxillary palp; mx, maxilla.
1438	Figure 4. Extant larvae of Bibionidae. (A–B) <i>Bibio varipies</i> Meigen, 1830, CeNak, no collection
1439	number assigned. (C) <i>Penthetria funebris</i> Meigen, 1804, ZSM, no collection number assigned.
1440	(A) habitus ventral. (B) head capsule, ventral. (C) head capsule of fourth instar larva, ventral.
1441	
1442	Figure 5 Extant larvae of Bibionidae. (A-C) Penthetria funebris Meigen, 1804, ZSM, no
1443	collection number assigned. A) fourth instar larva, habitus dorsal, arrows indicate the position of
1444	spiracles. (B) first instar larva, habitus ventral. (C) first instar larva, spiracle 1 (red arrow in B).
1445	
1446	Figure 6. Fossil dipteran larva, <i>Pachyneura</i> , collection of GPIH, accession number (L-7617). (A)
1447	habitus, dorsal. (B) schematic drawing of habitus, dorsal. a2–a8, abdominal segment 2–8; cl,
1448	clypeus; Abbreviations: hc, headcapsule; ms, mesothorax; mt, metathorax; pt, prothorax; s1–s10,
1449	spiracle 1–10.
1450	Figure 7 Fassil dinteren large Declaration of CDIII (I. 7617) (A) habitus ventral
1451 1452	Figure 7. Fossil dipteran larva, <i>Pachyneura</i> , collection of GPIH (L-7617). (A) habitus, ventral. (B) coloured version of A. Abbreviations: a1–a8, abdominal segments 1–8; c1–c6, creeping
1452	welts 1–6; hc, headcapsule; lb, labrum; md, mandibles; mp, maxillar palp; ms, mesothorax; mt,
1454	metathorax; mx, maxilla; pt, prothorax; te, trunk-end.
1455	metaliotax, mx, maxima, pt, productax, te, traine ena.
1456	Figure 8. Fossil dipteran larva, <i>Pachyneura</i> , collection of GPIH, accession number (L-7617). (A)
1457	head capsule, dorsal view. (B) head capsule, ventral view. (C) coloured version of B. (D) head
1458	capsule ventral view, schematic drawing. Abbreviations: hb, hypostomal bridge; hc, head
1459	capsule; lb, labrum; md, mandibles; mp, maxilarry palps; mx, maxillae.
1460	
1461	Figure 9. Fossil dipteran larva, Mycetobia, DEI, accession number Dip-00640. (A) habitus,
1462	dorsal view. (B) coloured version of A. (C) posterior spiracles, specimen 2 of B. (D) coloured



version of C. Abbreviations: a2–a8, abdominal segments 2–8; as, anterior spiracle; hc, head capsule; ms, mesothorax; mt, metathorax; ps, posterior spiracle; pt, prothorax.

1465

- 1466 Figure 10. Fossil dipteran larva, *Mycetobia*, DEI accession number Dip-00640, specimen 1 of
- 1467 Fig. 8B.(A) head capsule, dorsal view. (B) anterior spiracle. (C) coloured version of A. (D) head
- 1468 capsule, ventral view. (E) coloured version of D. Abbreviations: an, antenna; as, anterior
- spiracle; hc, head capsule; lb, labrum; md, mandibles; mn, mentum; mp, maxilar palps; mx,
- 1470 maxillae; ps, posterior spiracle.

1471

- 1472 Figure 11. Extant dipteran larva, *Mycetobia pallipes* Meigen, 1818, ZSM, no collection number
- 1473 assigned. (A) habitus, lateral. (B) coloured version of A. (C) head capsule, lateral view. (D)
- 1474 coloured version of C. Abbreviations: a2–a8, abdominal segment 2–8; as, anterior spiracle; hc,
- head capsule; md, mandible; mn, mentum; ms, mesothorax; mt, metathorax; mx, maxillae; pt,
- 1476 prothorax; tp, posterior pit of tentorium.

1477

- 1478 Figure 12. Fossil pupa, *Mycetobia connexa* (Mycetobia "morphotype 1"), GPIH, collection
- number 1851-DN. (A) habitus, ventro-lateral view. (B) coloured version of A. Abbreviations:
- 1480 a3–a7, abdominal segments 3–7; an, antennae; fs, frontal setae; p1, front legs; p2, midlegs; p3,
- 1481 hind legs; te. trunk-end; wn. wings.

1482

- 1483 Figure 13. Fossil pupa, *Mycetobia* "morphotype 2", PED, collection number PED-4866. (A)
- habitus, lateral view. (B) coloured version of A. Abbreviations: a1–a8, abdominal segments 1–8;
- an, antennae; ey, eyes; ms, mesothorax; mt, metathorax; p1, front legs; p2, midlegs; p, prothorax;
- 1486 te, trunk-end; th, thoracic horns; wn, wings.

1487

- 1488 Figure 14. Fossil pupa, *Mycetobia* "morphotype 3", pharate adult, DEI, collection number
- 1489 CCHH-DEI-608-2. (A) habitus, dorsal view. (B) habitus, ventral view.

1490

- 1491 Figure 15. Extant pupa, *Mycetobia pallipes* Meigen, 1818, ZSM, no collection number assigned,
- 1492 (A) habitus, dorsal view. (B) coloured version of A. (C) habitus, ventral view. (D) coloured
- version of C. Abbreviations: an-antennae; a3–a7, abdominal segments 3–7: ey, eyes; fs, frontal
- setae; mt, mesothorax; p1, front legs; p2, midlegs; p3, hind legs; te, trunk-end; th, thoracic horn;
- 1495 wn, wing.

1496

- 1497 Figure 16. Fossil larva, Sylvicola, DEI, collection number Dip-00642. (A) habitus, lateral view.
- 1498 (B) coloured version of A. (C) head capsule, lateral view. (D) coloured version of C.
- 1499 Abbreviations: a1–a8, abdominal segments 1–8; an, antennae; as, anterior spiracle; hc, head
- 1500 capsule; lb, labrum; md, mandible, mn, mentum; mx, maxilla; ms, mesothorax; te, trunk end.

1501

1502 Figure 17. Reconstructed ontogenetic sequence for representatives of *Mycetobia* in the Eocene.



1503	
1504	Figure 18. Summary of the statistical analysis. (A) biplot of fossil larvae of Mycetobia (n=36),
1505	head capsule length vs. head capsule width, red circles indicate hypothetical divisions into
1506	different larval stages based on the gaps in the data point distribution. I-IV, number of
1507	hypothetical larval stages. The number of specimens measured per stage is given at the plot; (B)
1508	distribution of the size cohorts within a sample of the fossil larvae of <i>Mycetobia</i> ; upper-rowleft,
1509	histogram of the head capsule width distribution (n=26); upper-row-center, histogram of the head
1510	capsule length distribution (n=25); upper-row right, histogram of the body length distribution
1511	(n=36); lower-row left, ranged plot (values ordered in ascending order) of the head capsule
1512	width, hypothetical division into different larval stages based on gaps in data point distribution
1513	indicated with I–IV as numbers of supposed larval stages; lower-row centered, ranged plot
1514	(values ordered in ascending order) of head capsule length; lower-row right, ranged plot (values
1515	ordered in ascending order) of body length.
1516	
1517	Figure 19. Natural logarithm of the mean larval head capsule width and head capsule of fossil
1518	larvae of <i>Mycetobia</i> , plotted against associated instar number. The fourth larval stage is
1519	represented by a single specimen, therefore the actual values are plotted instead of mean. Red
1520	dots and line representing the head capsule width, while blue represents the head capsule length.
1521	Error bars are representative of the value's standard deviation.
1522	
1523 1524	SUPPLEMENTARY FIGURES
1525	Figure S1. Fossil larva, holotype of <i>Dinobibio hoffeinseorum</i> sp. nov. GPIH, accession number
1526	(GPIH-0024). (A) ventro-lateral view. (B) dorso-lateral view; (C1–C2) spiracle 10. (D1–D2)
1527	spiracle 2. (E1–E2) spiracle 1.
1528	Spiracle 2. (E1 E2) spiracle 1.
1529	Figure S2. Fossil larvae, <i>Mycetobia</i> with syninclusions, GPIH, collection number GPIH-0247.
1530	(A) overview of the amber piece. (B) caddisfly male, Polycentropodidae. (C) partial syninclusion
1531	of an adult beetle. 1–4, larvae of <i>Mycetobia</i> ; 5, beetle; 6–10 larvae of <i>Mycetobia</i> ; 11, caddisfly
1532	male, Polycentropodidae
1533	
1534	Figure S3. Fossil larvae, <i>Mycetobia</i> with syninclusions, collection number Dip-00640. (A)
1535	Overview of the inclusions. (B–D) dipterans, non-biting midges (Chironomidae). (B)
1536	Rheosmittia pertenuis, male. (C) Orthocladiinae, female. (D) Rheosmittia pertenuis, male,
1537	second specimen. (E) partial inclusions of <i>Mycetobia</i> sp. larvae. 1–4 Mycetobia larvae; 5–6 R.
1538	pertenuis, males; 7 Orthocladiinae, female.
1539	
1540	Figure S4. Fossil larvae, Mycetobia, DEI, collection number Dip-00639. (A) habitus. (B) trunk
1541	end, with posterior spiracles. (C) head capsule, ventral view.



- 1543 Figure S5. Fossil larvae, *Mycetobia*. (A) PED-5695. (B) DEI, collection number Dip-00654. (C)
- 1544 GPIH (BI-2350). (D) PED-4965.

- 1546 Figure S6. Fossil larva, *Mycetobia* with syninclusions, collection of GPIH, collection number
- 1547 3706-W. (A) mite. (B) fly, Phroidae. (C, D) larval specimen of *Mycetobia*. (C) ventral view. (D)
- 1548 dorsal view.

1549

- 1550 Figure S7. Fossil larvae, Mycetobia. A) Two specimens, GPIH (L-7592). (B) two specimens,
- 1551 GPIH (L-7592). (C) four specimens (1–4), PED, collection number PED-4748. (D) larva with
- 1552 syninclusions, PED, collection number PED-4970. 1, scale insect, (Coccoidea), nymph; 2, leaf
- hopper (Cicadellidae), nymph; 3, larva, *Mycetobia*; 4, non-biting midge (Chironomidae), female.

1554

- 1555 Figure S8. Fossil larvae, *Mycetobia*, DEI, collection number Dip-00649. (A) large larva. (B)
- 1556 specimens 1–3. (C) large larva.

1557

- 1558 Figure S9. Fossil larvae, *Mycetobia* with syninclusions. A) Overview of the amber piece Dip-
- 1559 00656 from the collection of DEI. (B–D) larvae, Mycetobia. (B) specimen 1. (C) specimen 2. (D)
- 1560 specimen 3. 1, 2, 5, larva, Mycetobia; 3, 8, 10, 14 gall midges (Cecidomyiidae); 4, mite (Acari);
- 1561 6, fly ("Acalyptrata"); 7, beetle (Coleoptera); 9, 11–13, ants (Fromicidae).

1562

- 1563 Figure S10. Fossil larvae, *Mycetobia*, DEI, collection number Dip-00655. (A) specimen 1. (B)
- specimen 2.

1565

- 1566 Figure S11. Fossil pupa (exuvium), *Mycetobia* "morphotype 1" with syninclusions, collection
- number PED-4395. (A) pupal exuvim of *Mycetobia* "morphotype 1". (B) *Mycetobia connexa*,
- 1568 female. (C) partial beetle (Coleoptera).

1569

- 1570 Figure S12. Fossil pupa, *Mycetobia connexa (Mycetobia* "morphotype 1"), GPIH collection
- number AKBS-00071. (A) habitus, ventro-lateral view. (B) abdomen, dorsal view.

1572

- 1573 Figure S13. Fossil pupa, *Mycetobia* "morphotype 1" with syninclusions, DEI, collection number
- 1574 Dip-00651. (A) habitus, lateral view. (B) dipteran non-biting midge (Chrionomidae,
- 1575 Orthocladiinae). (C) fly (Sciaroidea).

1576

- 1577 Figure S14. Fossil pupa, *Mycetobia connexa* (*Mycetobia* "morphotype 1") with syninclusions,
- 1578 GPIH, collection number 1851-DN. (A) pupa (exuvium), *Mycetobia* "morphotype 1" and fungus
- gnat (Keroplatidae) male. (B) fly (Sciaridae) male. (C) fly (Bibionomorpha, probably
- 1580 Anisopodidae).



- 1582 Figure S15. Fossil pupa (exuvium), *Mycetobia connexa* (*Mycetobia* "morphotype 1") with
- syninclusions, collection number PED-4395. (A) Overview. (B) *Mycetobia connexa* male. (C)
- 1584 Mycetobia connexa male, distal part of metathoracic tibia. 1, Mycetobia connexa male; 2,
- 1585 *Mycetobia connexa* female; 3, pupal exuvium of *M. connexa*.

- 1587 Figure S16. Fossil pupae, *Mycetobia* "morphotype 1". (A) DEI, collection number Dip-00657,
- dorsal view. (B) DEI, collection number Dip-00659, lateral view.

1589

- 1590 Figure S17. Fossil pupa, *Mycetobia* "morphotype 1", DEI, collection number Dip-00657
- 1591 (Bitterfeld amber). (A) habitus, dorsal view. (B) habitus, ventral view.

1592

- 1593 Figure S18. Fossil pupa, *Mycetobia* "morphotype 1", DEI, collection number Dip-00655. (A)
- habitus, dorsal view. (B) habitus, ventro-lateral view.

1595

- 1596 Figure S19. Fossil pupa, *Mycetobia* "morphotype 1" with syninclusion, DEI, collection number
- 1597 Dip-00655 (specimen 2). (A) habitus, lateral view. (B) habitus, ventro-lateral view. (C) fly
- 1598 (Diptera, Sciaridae).

1599

- 1600 Figure S20. Fossil pupa (exuvium), *Mycetobia* "morphotype 1" collection number PED-4998.
- 1601 (A) habitus, ventral view. (B) habitus, dorsal view.

1602

- 1603 Figure S21. Fossil pupa (exuvium), *Mycetobia* "morphotype 1" (Bitterfeld amber), collection
- number Dip-00661. (A) habitus, ventral view. (B) habitus, dorsal view, (C) habitus, lateral view.

1605

- 1606 Figure S22. Fossil pupa, *Mycetobia* "morphotype 1" (Bitterfeld amber), DEI, collection number
- 1607 Dip-00650 . (A) habitus, dorsal view. (B) habitus, ventral view.

1608

- 1609 Figure S23. Fossil pupa, *Mycetobia* "morphotype 1" and syninclusions, GPIH, N-7095. A)
- overview. (B) pupa (upper left) *Mycetobia* "morphotype 1", (upper left) and larva of Neuroptera;
- lower right). (C, D) adult long-legged fly (Dolichopodidae). (C) specimen 1 (D) specimen 2.

1612

- 1613 Figure S24. Fossil pupa (exuvium), *Mycetobia* "morphotype 1", DEI, collection number Dip-
- 1614 00653. (A) habitus, dorsal view. (B) habitus, ventral view. (C) habitus, lateral view.

1615

- 1616 Figure S25. Fossil pupa (exuvium), *Mycetobia* "morphotype 1", rendering of u-CT scans, DEI,
- 1617 collection number Dip-00653. (A) habitus, dorsal view. (B) habitus, ventral view. (C) habitus,
- 1618 lateral view.

- 1620 Figure S26. Fossil pupa (exuvium), *Mycetobia* "morphotype 1", rendering of μ-CT scans,
- 1621 MfNB, collection number MB.I.7295 (A) habitus, dorsal view. (B) habitus, lateral view.

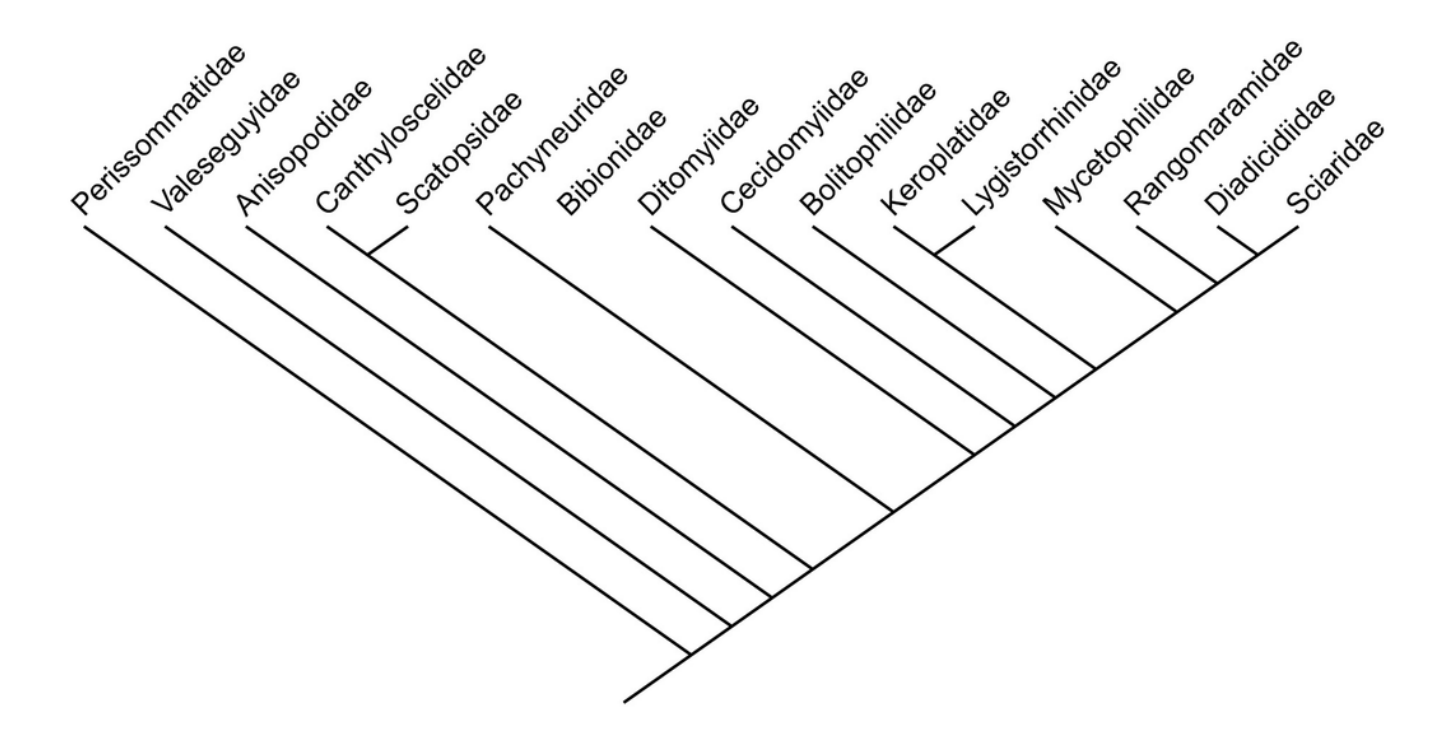




1622	(C) habitus, ventral view. (D) habitus, lateral view. All images red-blue stereo anaglyphs, please
1623	use red-cyan glasses to view.
1624	
1625	Figure S27. Fossil pupae, Mycetobia and syninclusions. (A)"morphotype 1" and syninclusions,
1626	GPIH, collection number AKBS-00071. 1, largely unidentifiable (Insecta); 2, 3, 5–9, 13, 15 ant
1627	worker (Lasius schiefferdeckeri Mayr, 1868); 4, Fossil pupa, Mycetobia "morphotype 1"; 10 ant
1628	worker (Ctenobethylus goepperti (Mayr, 1868)). (B) syninclusions to "morphotype 2", PED,
1629	collection number PED-4866; adult rove beetle (Coleoptera: Staphylinidae), two adult gall
1630	midges (Diptera; Cecidomyiidae). (C) pupa of Mycetobia "morphotype 2", GPIH, collection
1631	number L-7514, habitus, ventral view.
1632	
1633	Figure S28. Fossil pupa (pharate adult), <i>Mycetobia</i> "morphotype 3", rendering of μ-CT scans,
1634	DEI, collection number Dip-00660. (A) habitus, lateral view, right body side, mirrored. (B)
1635	habitus, lateral view, left body side. (C) habitus, dorsal view. (D) habitus, ventral view.
1636	
1637	Figure S29. Fossil pupa (pharate adult), Mycetobia "morphotype 3" DEI, collection number Dip-
1638	00652. (A) habitus, dorsal view. (B) habitus, ventral view.
1639	
1640	



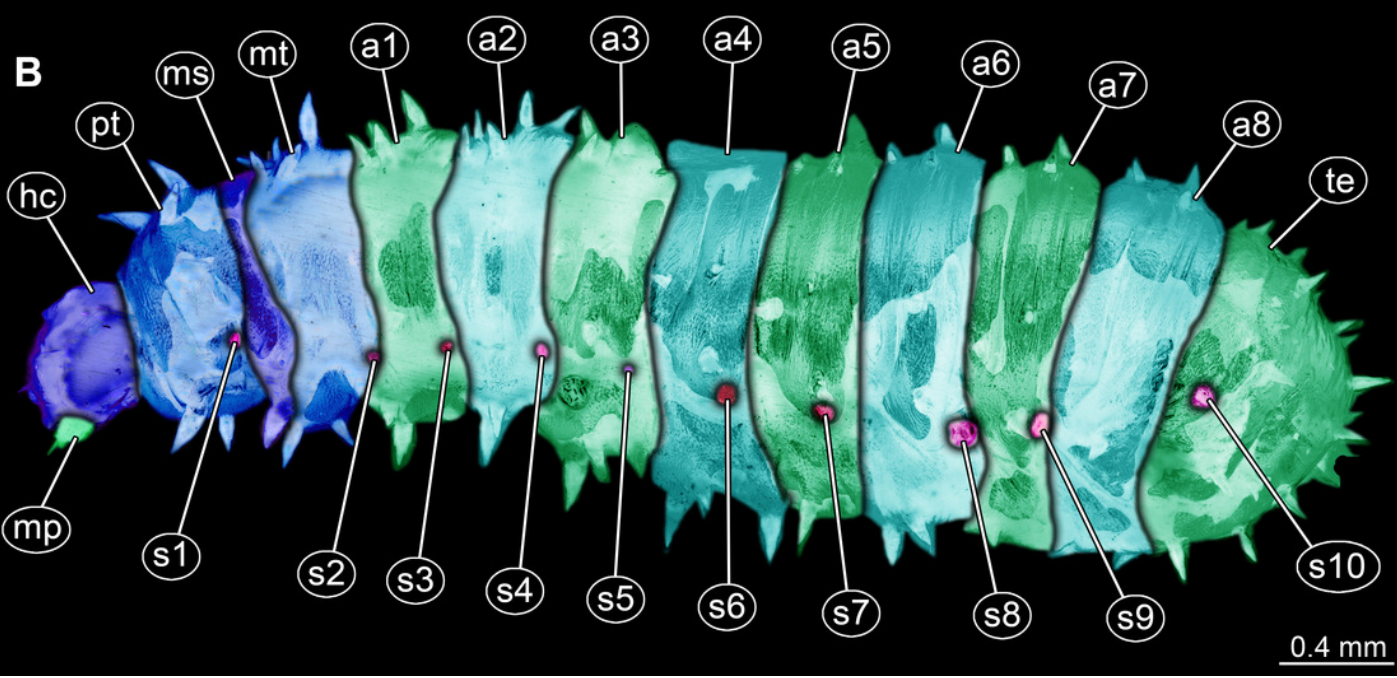
Phylogenetic relationship among different lineages of Bibionomorpha sensu lato, modified from Sevcik et al., 2016.



Dipteran larva, holotype of *Dinobibio hoffeinseorum* sp.n. GPIH, accession number (GPIH-0024) in lateral view.

(A) overview, composite image. (B) coloured version of A above. Abbreviations: a1-a8, abdominal segment 1-8; hc, head capsule; mp, maxillary process; ms, mesothorax; mt, metathorax, pt, prothorax; s1-s10, spiracle 1-10; te, trunk end.

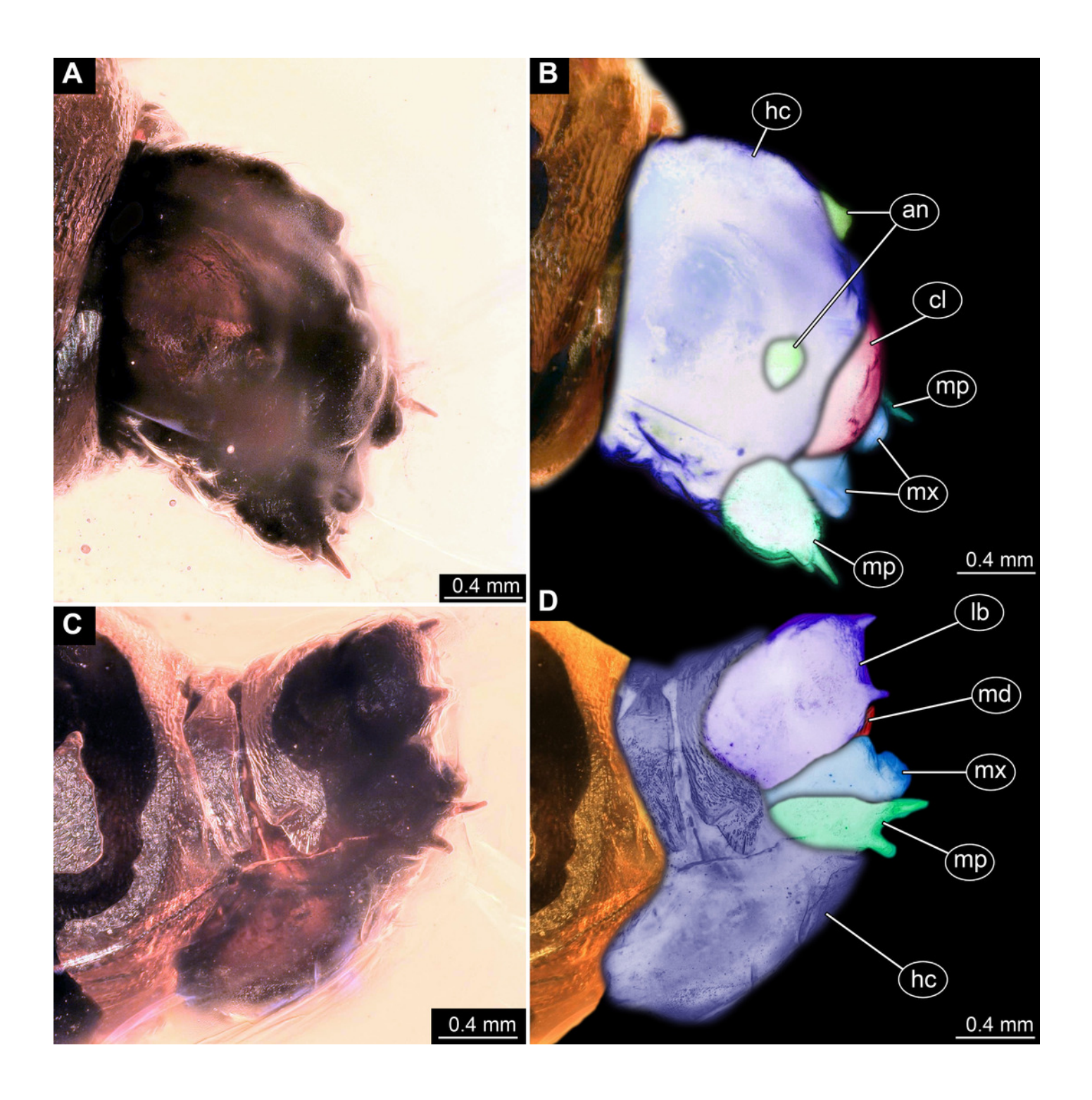






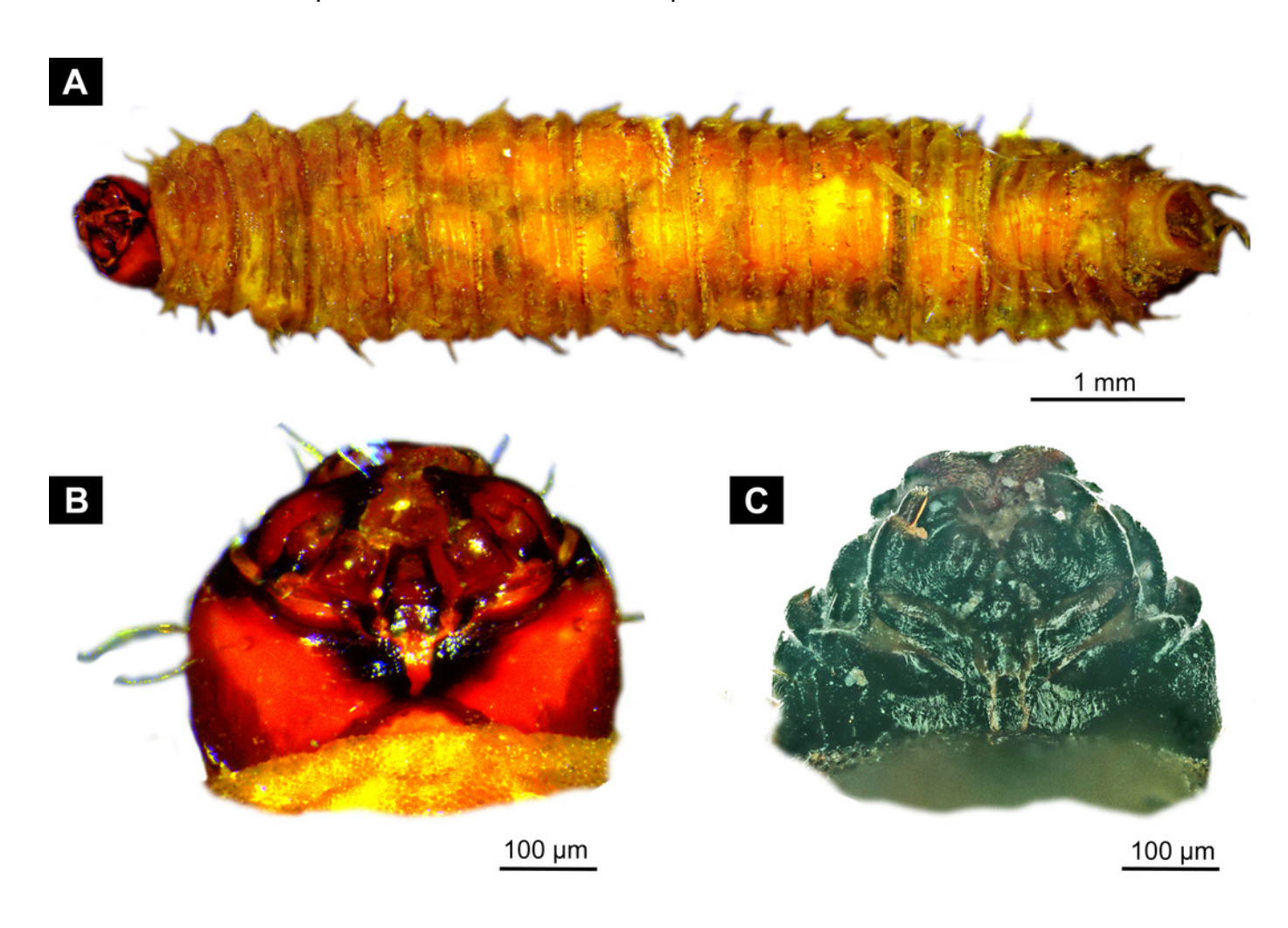
Fossil dipteran larva, holotype of *Dinobibio hoffeinseorum* sp.n. GPIH, accession number (GPIH-0024).

(A) head capsule, latero-dorsal view; (B) coloured version of A. (C) head capsule, ventrolateral view. (D) coloured version of C. Abbreviations: an, antennae; cl, clypeus; hc, head capsule; lb, labium; md, mandible; mp, maxillary palp; mx, maxilla.



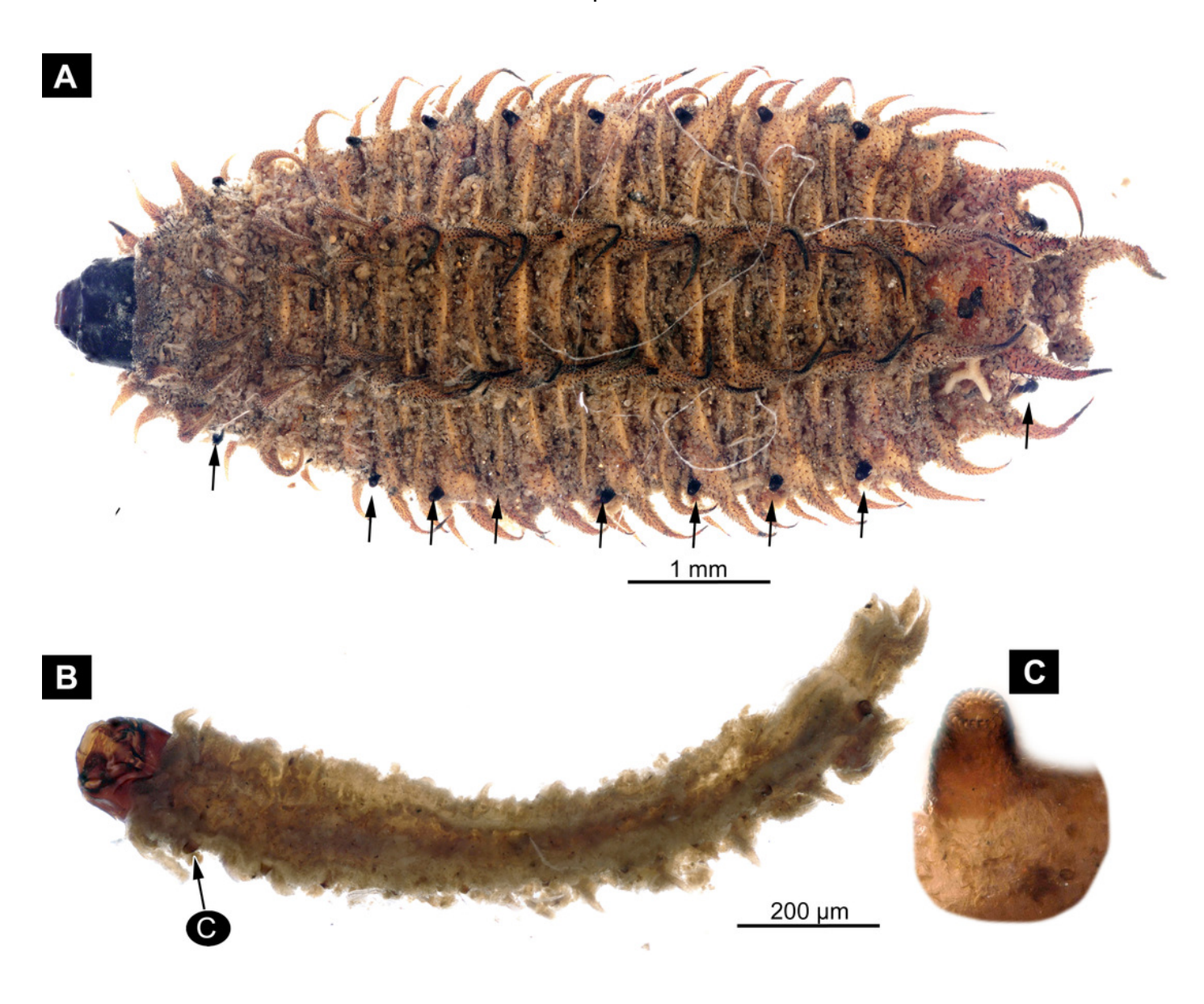
Extant larvae of Bibionidae. (A-C) *Bibio varipies* Meigen, 1830, CeNak, no collection number assigned.

(A) *Penthetria funebris* Meigen, 1804, ZSM, no collection number assigned. (A) habitus ventral. (B) head capsule, ventral. (C) head capsule of fourth instar larva, ventral.



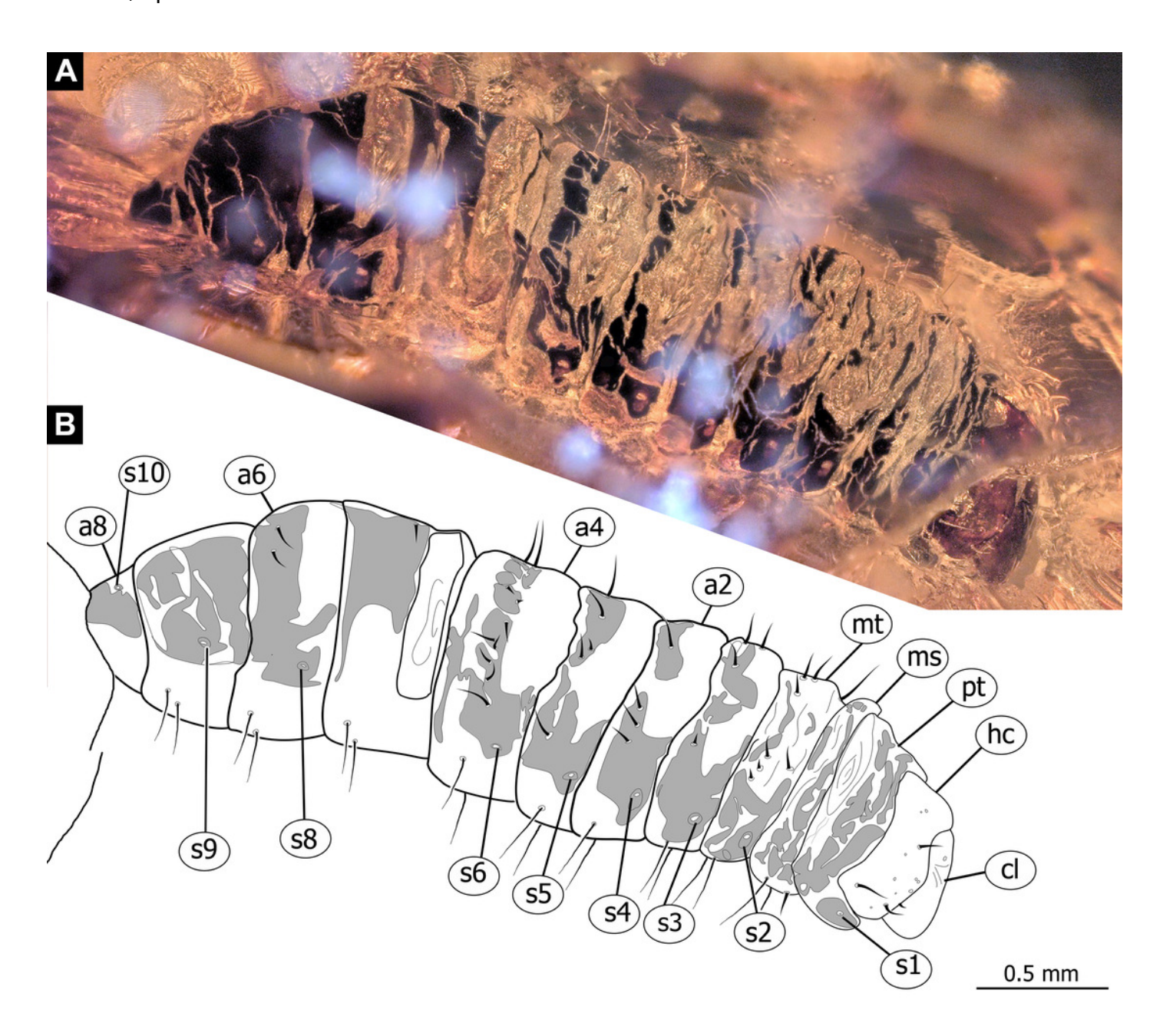
Extant larvae of Bibionidae. (A-C) *Penthetria funebris* Meigen, 1804, ZSM, no collection number assigned.

A) fourth instar larva, habitus dorsal, arrows indicate the position of spiracles. (B) first instar larva, habitus ventral. (C) first instar larva, spiracle 1 (red arrow in B).



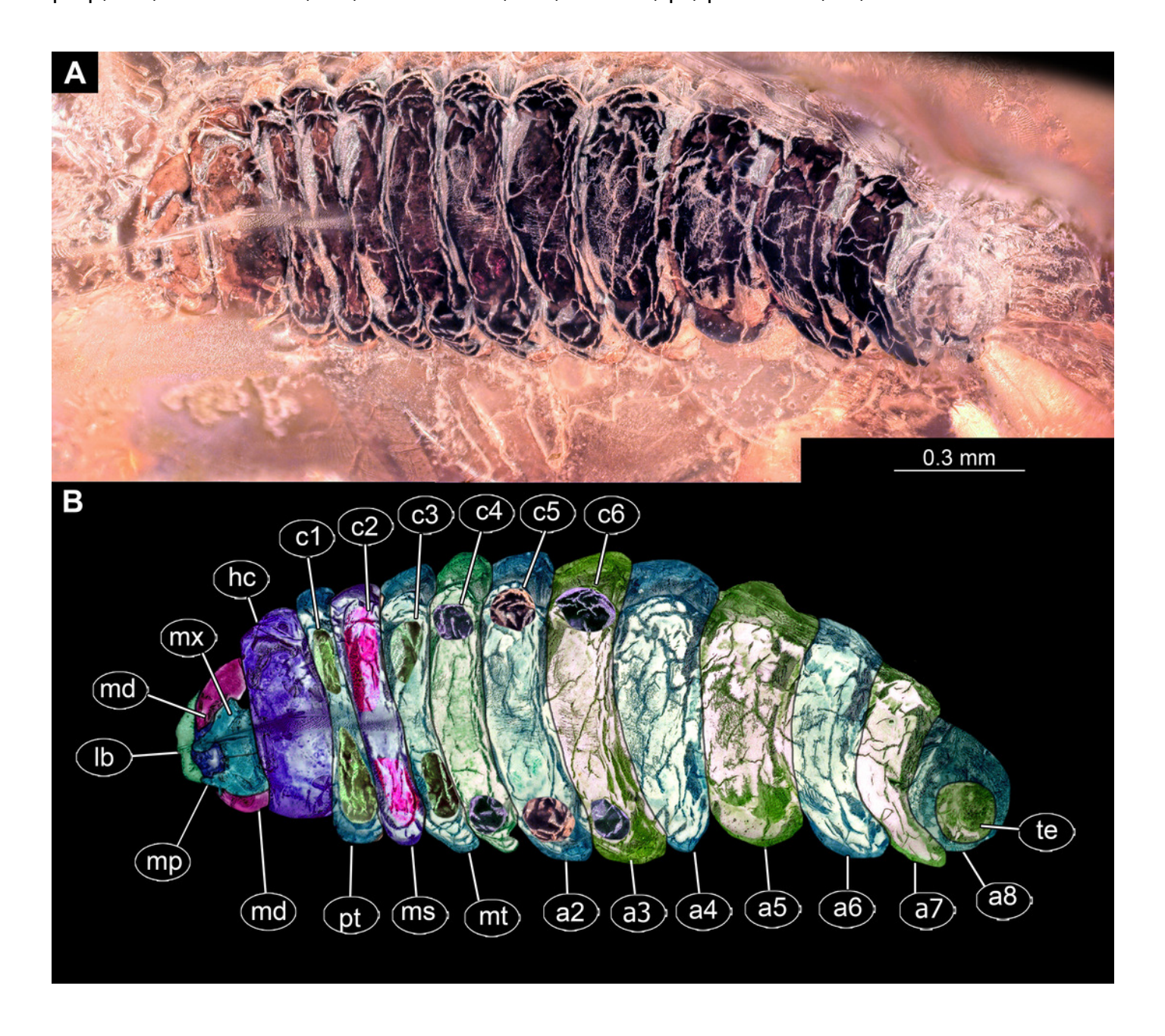
Fossil dipteran larva, Pachyneura, collection of GPIH, accession number (L-7617).

(A) habitus, dorsal. (B) schematic drawing of habitus, dorsal. a2-a8, abdominal segment 2-8; cl, clypeus; Abbreviations: hc, headcapsule; ms, mesothorax; mt, metathorax; pt, prothorax; s1-s10, spiracle 1-10.



Fossil dipteran larva, Pachyneura, collection of GPIH (L-7617).

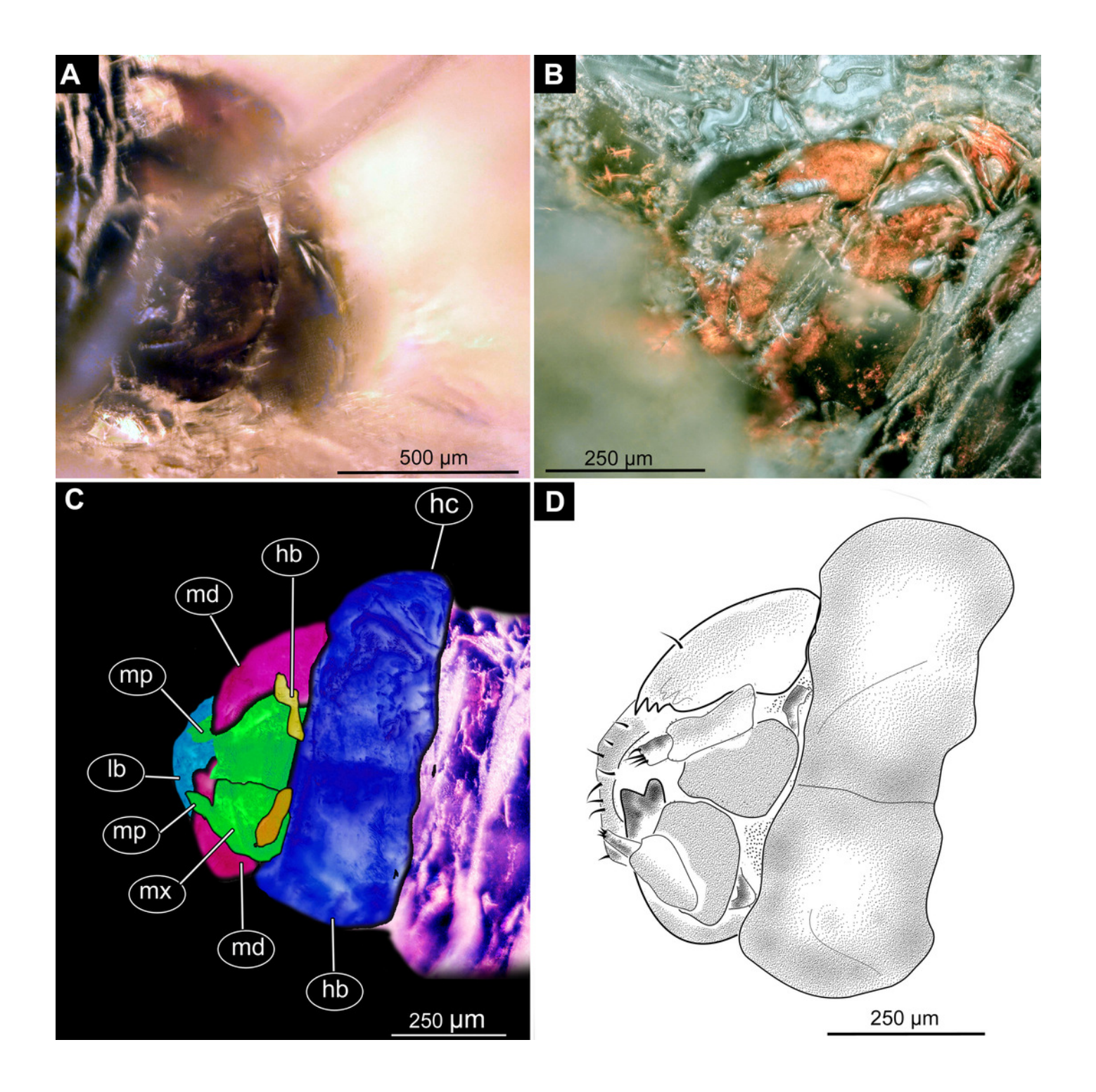
(A) habitus, ventral. (B) coloured version of A. Abbreviations: a1-a8, abdominal segments 1-8; c1-c6, creeping welts 1-6; hc, headcapsule; lb, labrum; md, mandibles; mp, maxillar palp; ms, mesothorax; mt, metathorax; mx, maxilla; pt, prothorax; te, trunk-end.





Fossil dipteran larva, Pachyneura, collection of GPIH, accession number (L-7617).

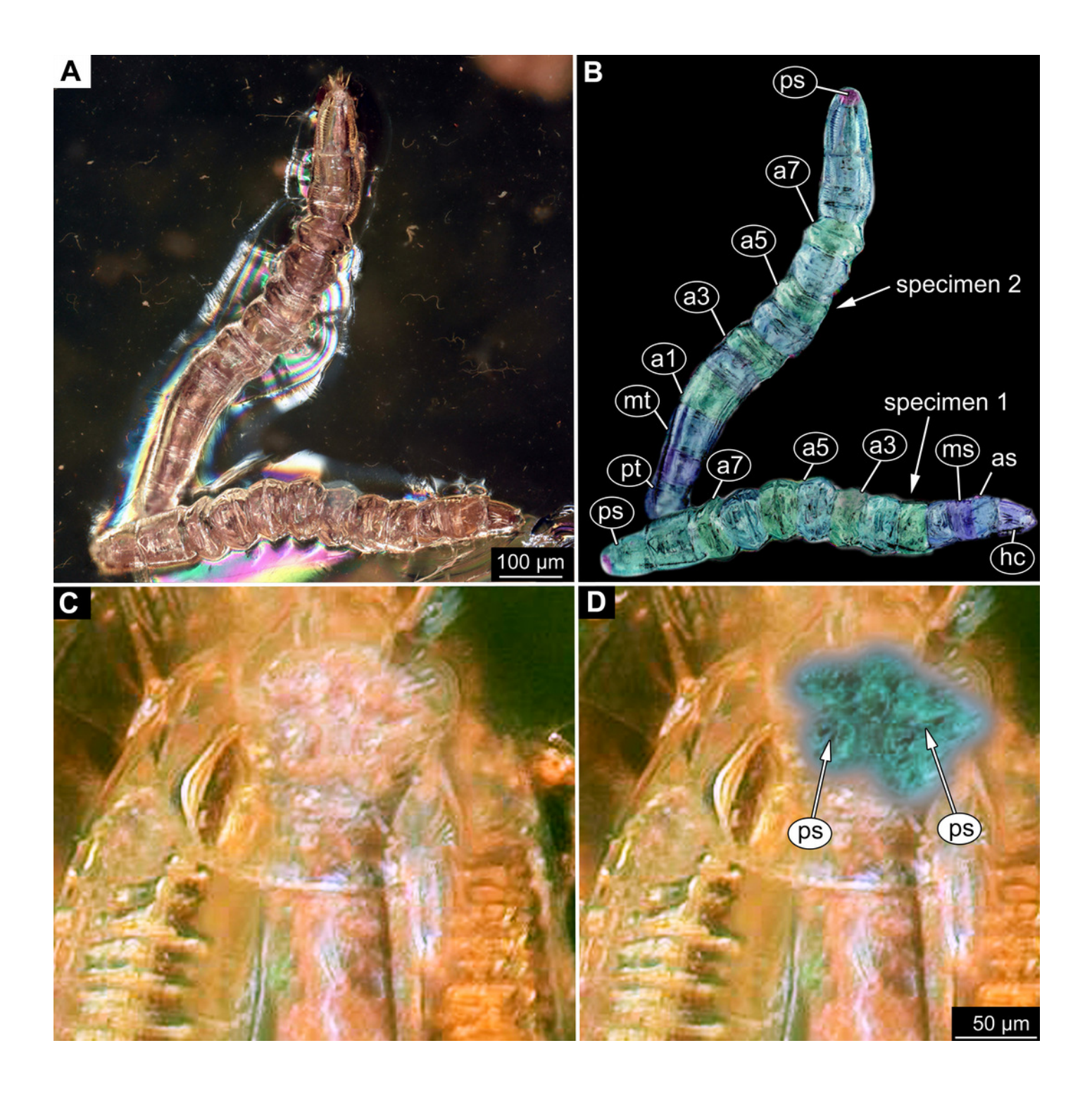
(A) head capsule, dorsal view. (B) head capsule, ventral view. (C) coloured version of B. (D) head capsule ventral view, schematic drawing. Abbreviations: hb, hypostomal bridge; hc, head capsule; lb, labrum; md, mandibles; mp, maxilary palps; mx, maxillae.





Fossil dipteran larva, Mycetobia, DEI, accession number Dip-00640.

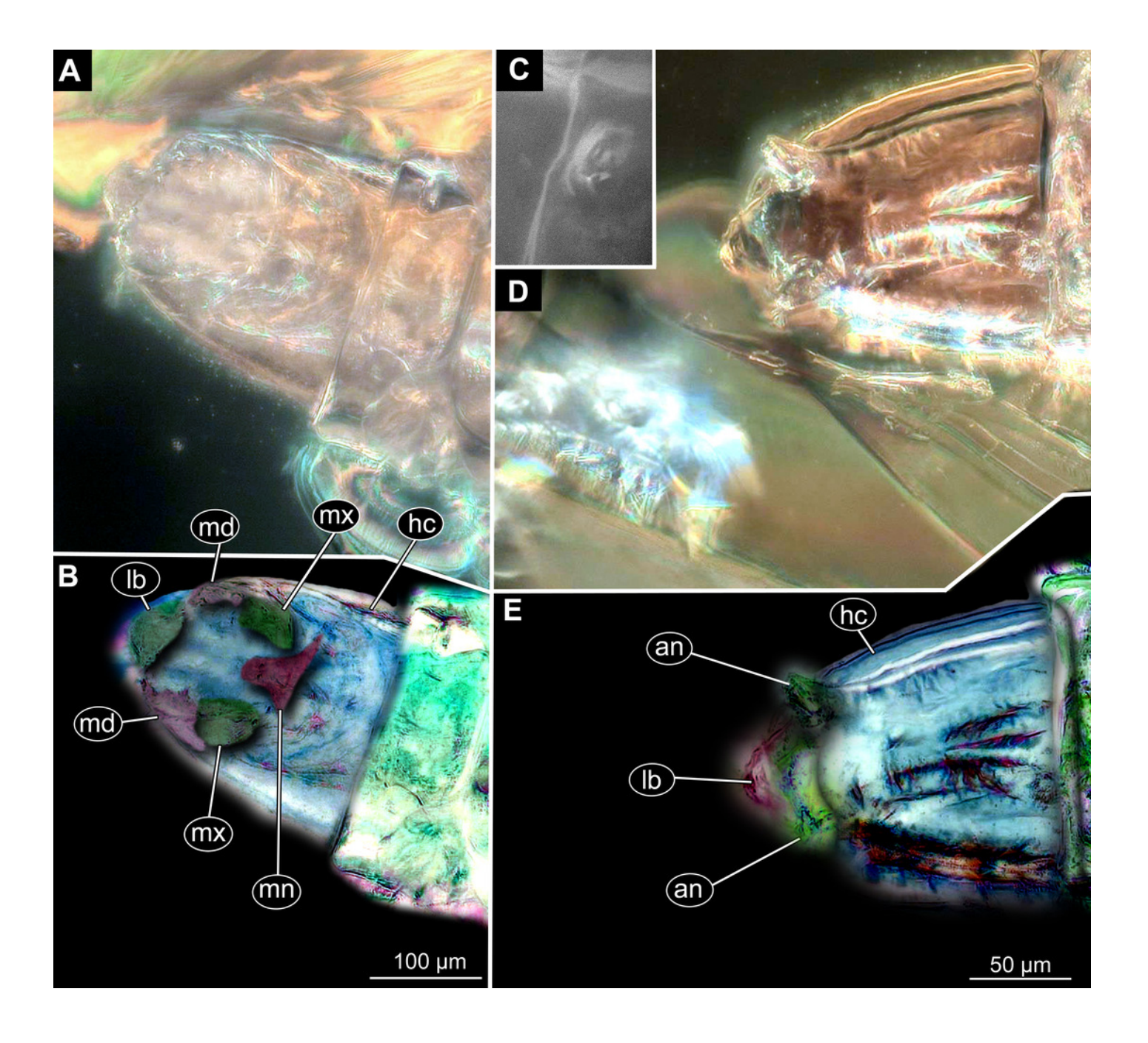
- (A) habitus, dorsal view. (B) coloured version of A. (C) posterior spiracles, specimen 2 of B.
- (D) coloured version of C. Abbreviations: a2–a8, abdominal segments 2–8; as, anterior spiracle; hc, head capsule; ms, mesothorax; mt, metathorax; ps, posterior spiracle; pt, prothorax.





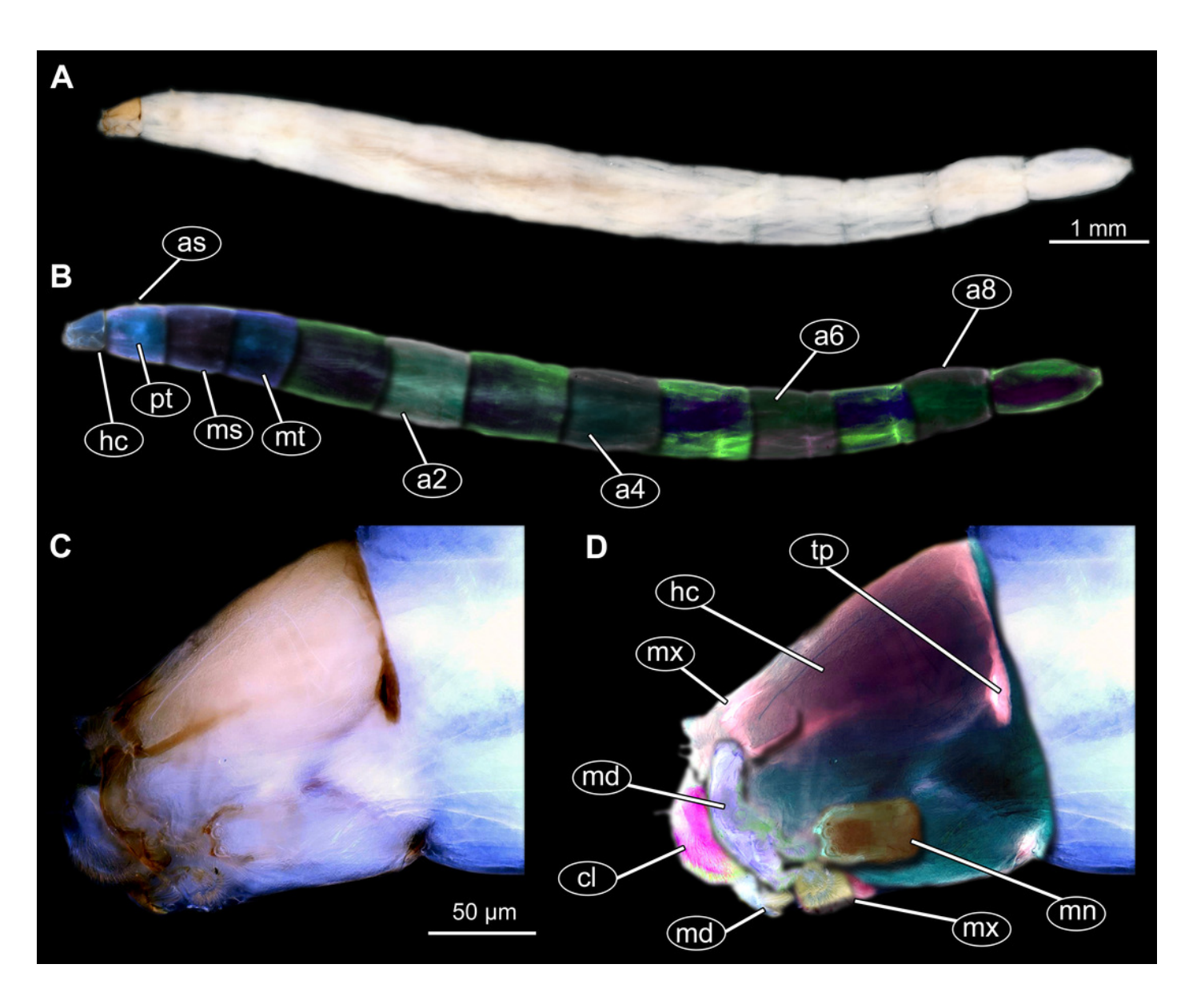
Fossil dipteran larva, *Mycetobia*, DEI accession number Dip-00640, specimen 1 of Fig. 8B.

(A) head capsule, dorsal view. (B) anterior spiracle. (C) coloured version of A. (D) head capsule, ventral view. (E) coloured version of D. Abbreviations: an, antenna; as, anterior spiracle; hc, head capsule; lb, labrum; md, mandibles; mn, mentum; mp, maxilar palps; mx, maxillae; ps, posterior spiracle.



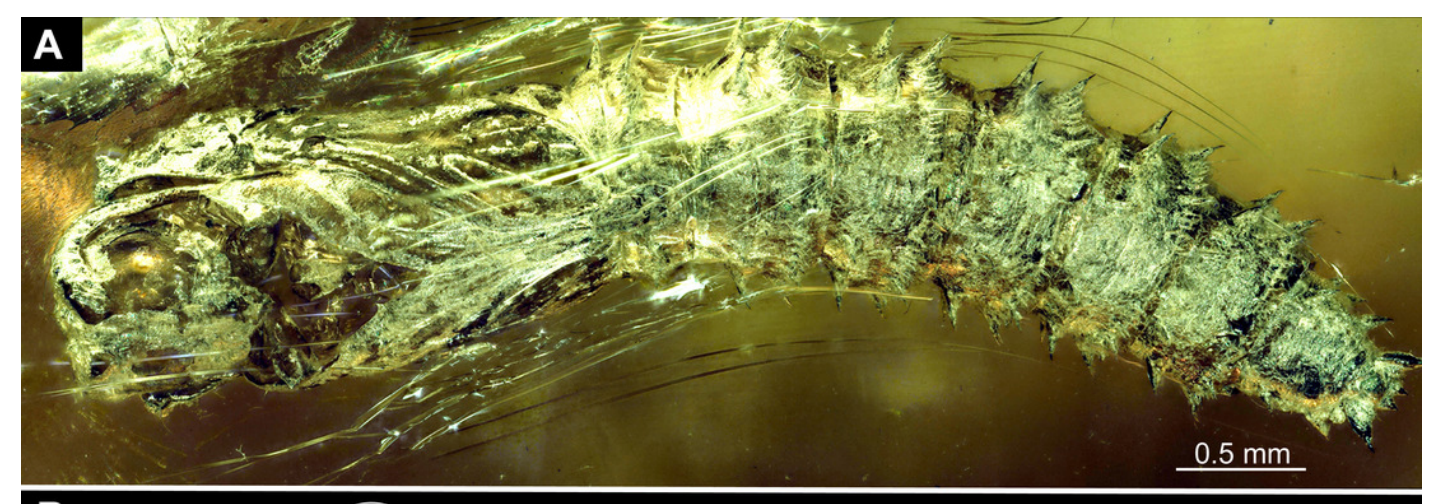
Extant dipteran larva, *Mycetobia pallipes* Meigen, 1818, ZSM, no collection number assigned.

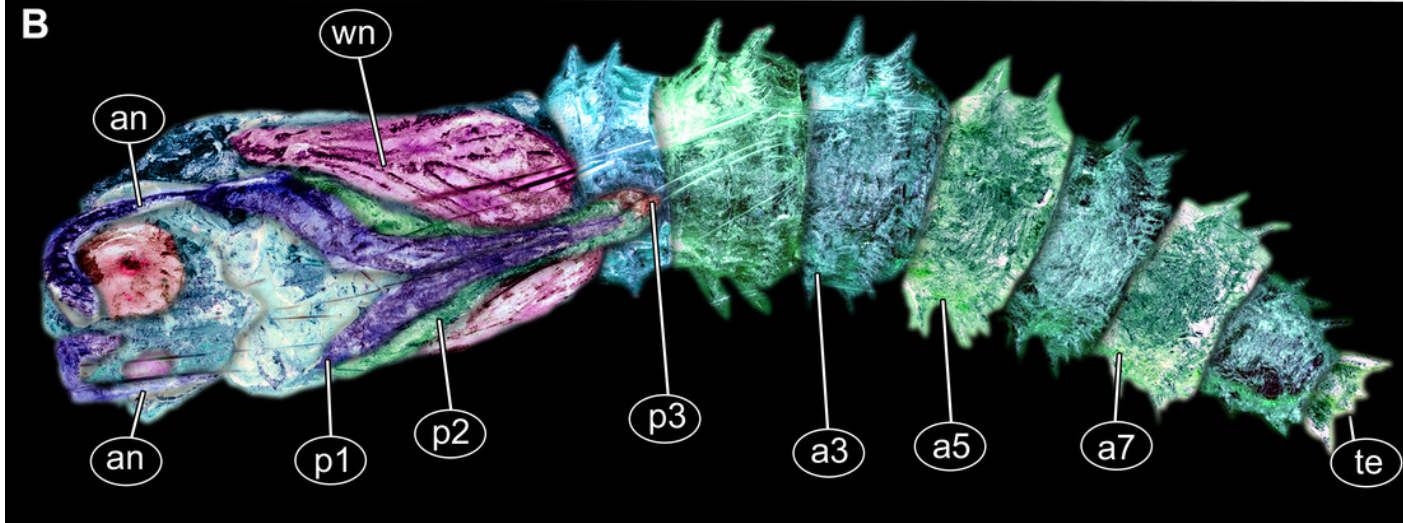
(A) habitus, lateral. (B) coloured version of A. (C) head capsule, lateral view. (D) coloured version of C. Abbreviations: a2–a8, abdominal segment 2–8; as, anterior spiracle; hc, head capsule; md, mandible; mn, mentum; ms, mesothorax; mt, methathorax; mx, maxillae; pt, prothorax; tp, posterior pit of tentorium.



Fossil pupa, *Mycetobia connexa* (Mycetobia "morphotype 1"), GPIH, collection number 1851-DN.

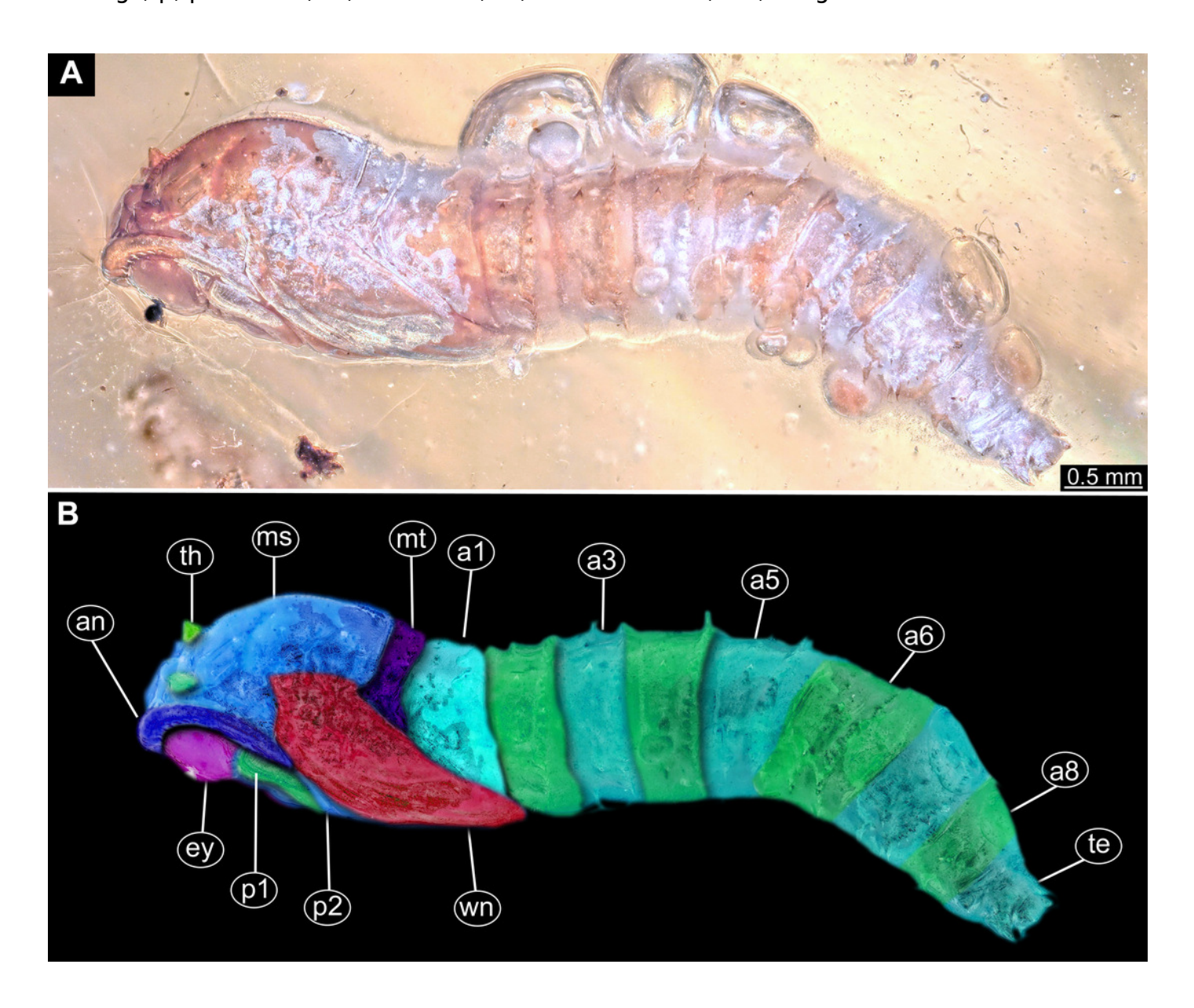
(A) habitus, ventro-lateral view. (B) coloured version of A. Abbreviations: a3–a7, abdominal segments 3–7; an, antennae; fs, frontal setae; p1, front legs; p2, midlegs; p3, hind legs; te, trunk-end; wn, wings.





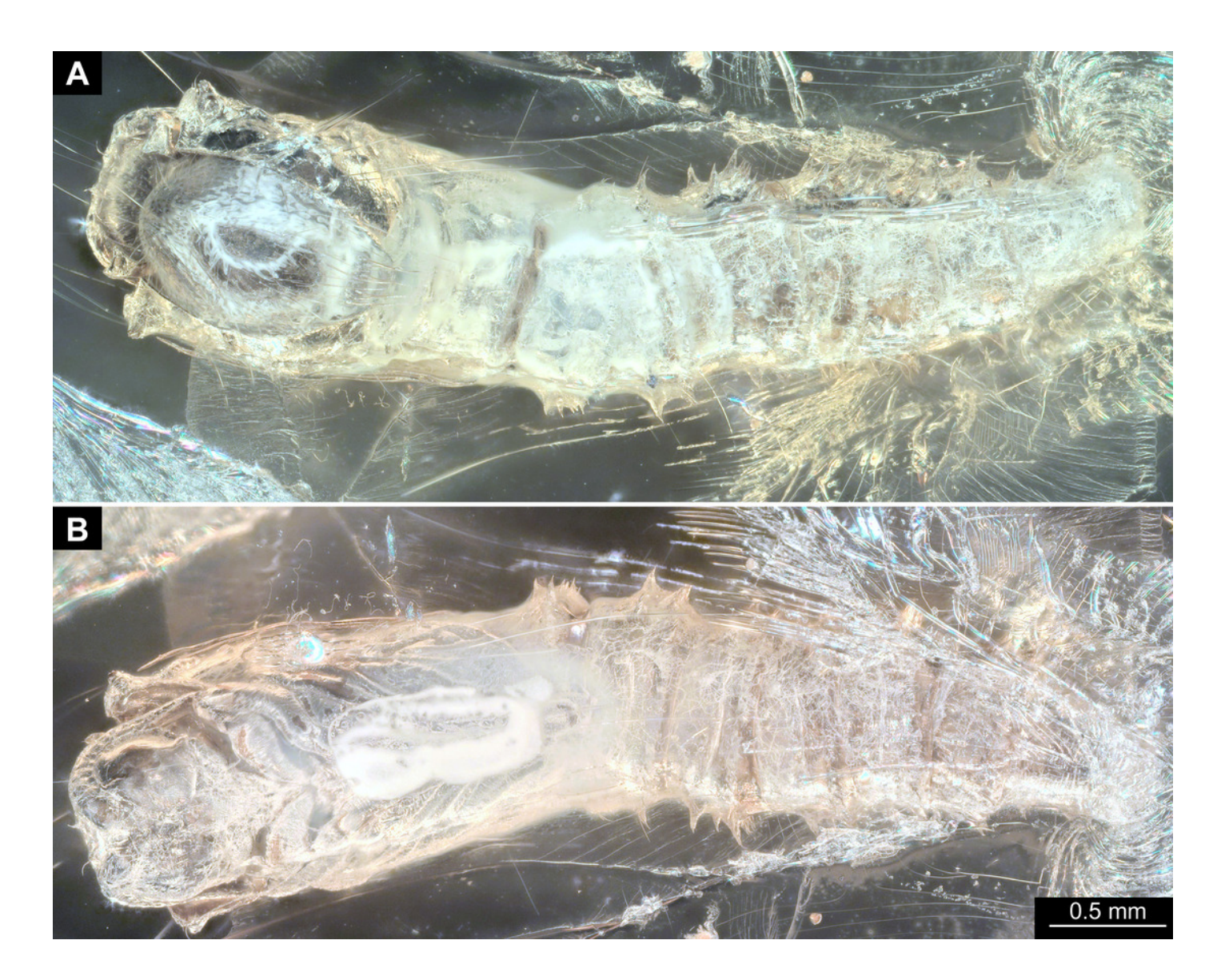
Fossil pupa, Mycetobia "morphotype 2", PED, collection number PED-4866.

(A) habitus, lateral view. (B) coloured version of A. Abbreviations: a1-a8, abdominal segments 1-8; an, antennae; ey, eyes; ms, mesothorax; mt, metathorax; p1, front legs; p2, midlegs; p, prothorax; te, trunk-end; th, thoracic horns; wn, wings.



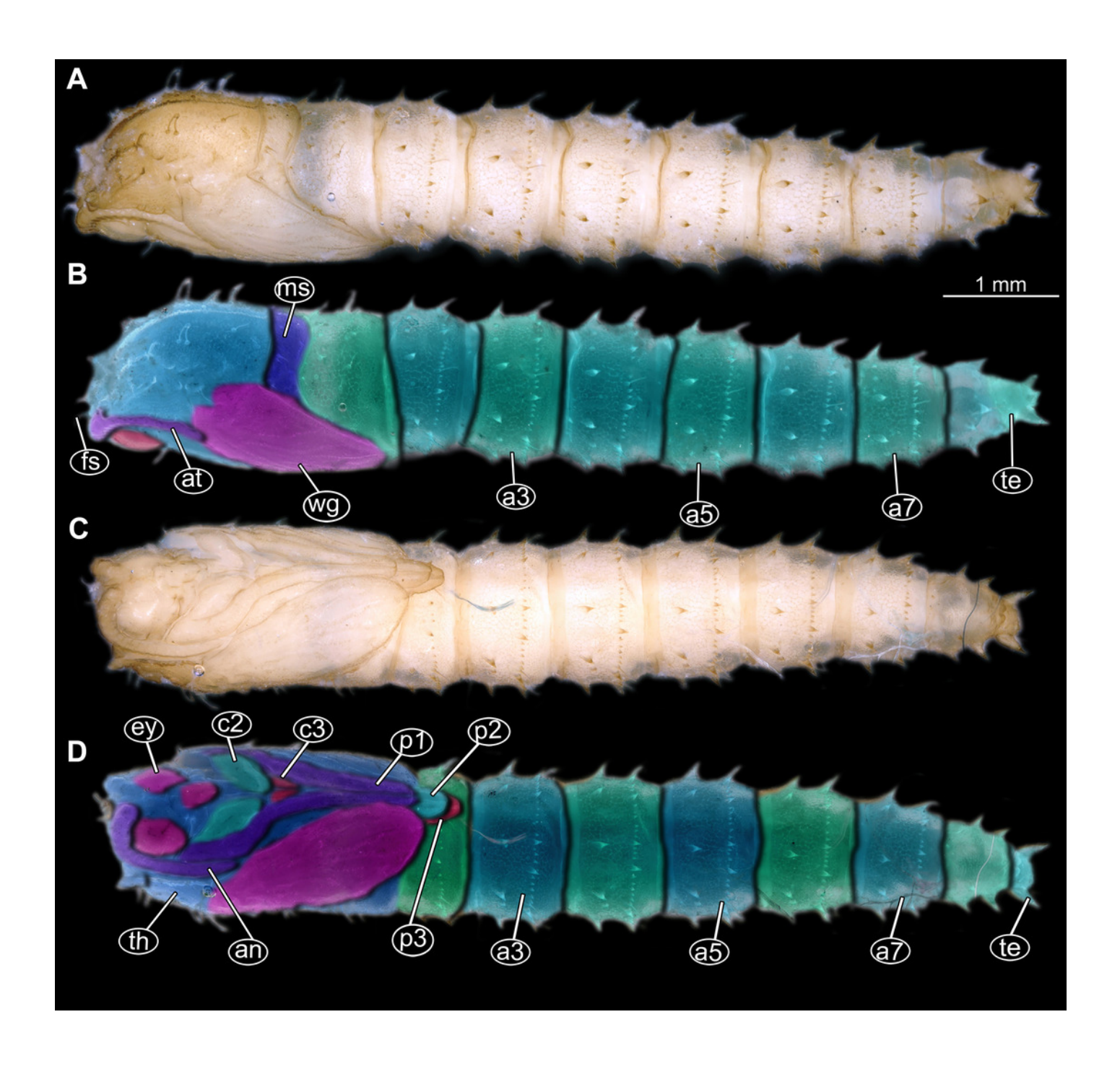
Fossil pupa, *Mycetobia* "morphotype 3", pharate adult, DEI, collection number CCHH-DEI-608-2.

(A) habitus, dorsal view. (B) habitus, ventral view.



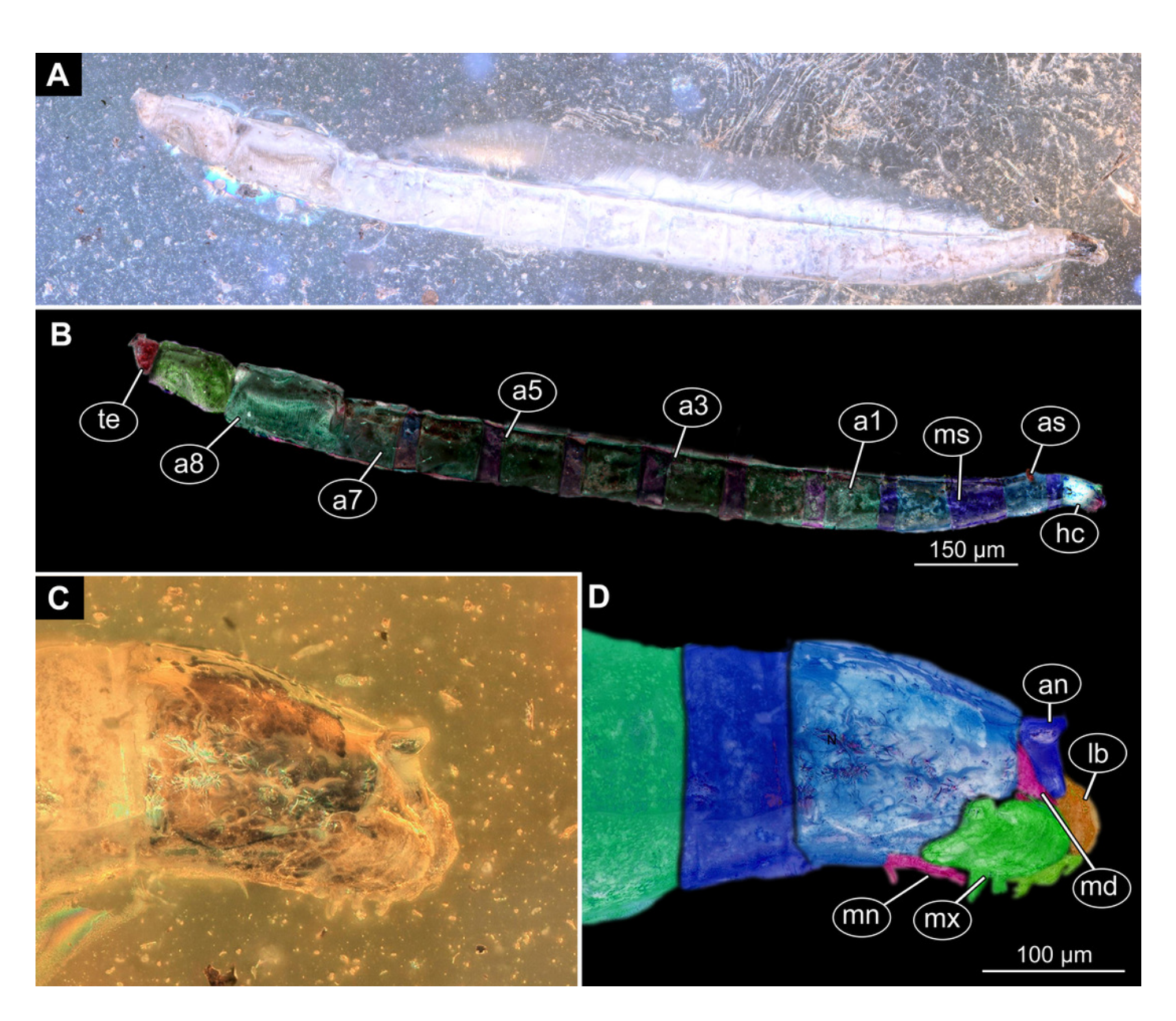


Extant pupa, *Mycetobia pallipes* Meigen, 1818, ZSM, no collection number assigned (A) habitus, dorsal view. (B) coloured version of A. (C) habitus, ventral view. (D) coloured version of C. Abbreviations: an-antennae; a3–a7, abdominal segments 3–7: ey, eyes; fs, frontal setae; mt, mesothorax; p1, front legs; p2, midlegs; p3, hind legs; te, trunk-end; th, thoracic horn; wn, wing.

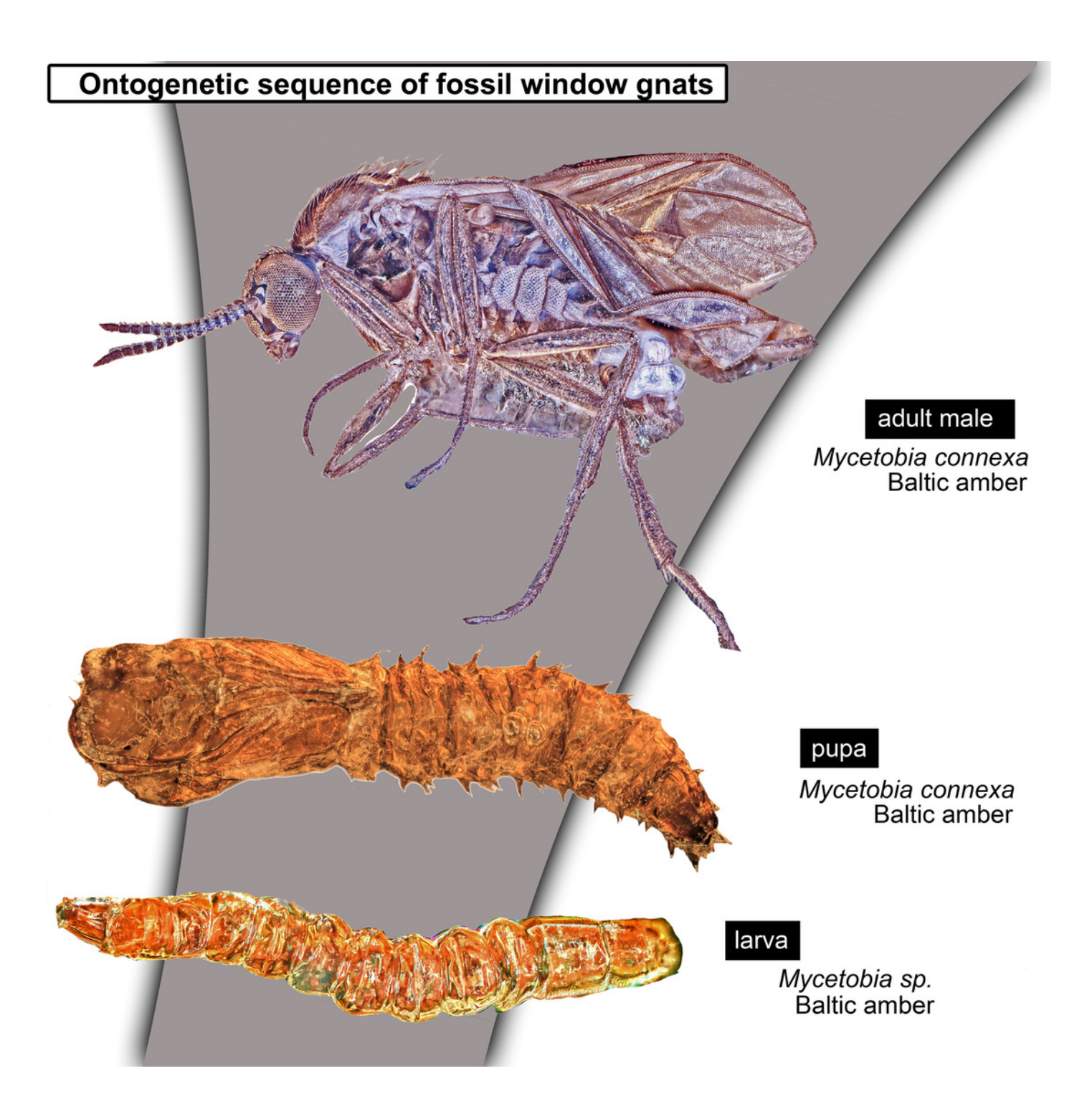


Fossil larva, Sylvicola, DEI, collection number Dip-00642.

(A) habitus, lateral view. (B) coloured version of A. (C) head capsule, lateral view. (D) coloured version of C. Abbreviations: a1–a8, abdominal segments 1–8; an, antennae; as, anterior spiracle; hc, head capsule; lb, labrum; md, mandible, mn, mentum; mx, maxilla; ms, mesothorax; te, trunk end.



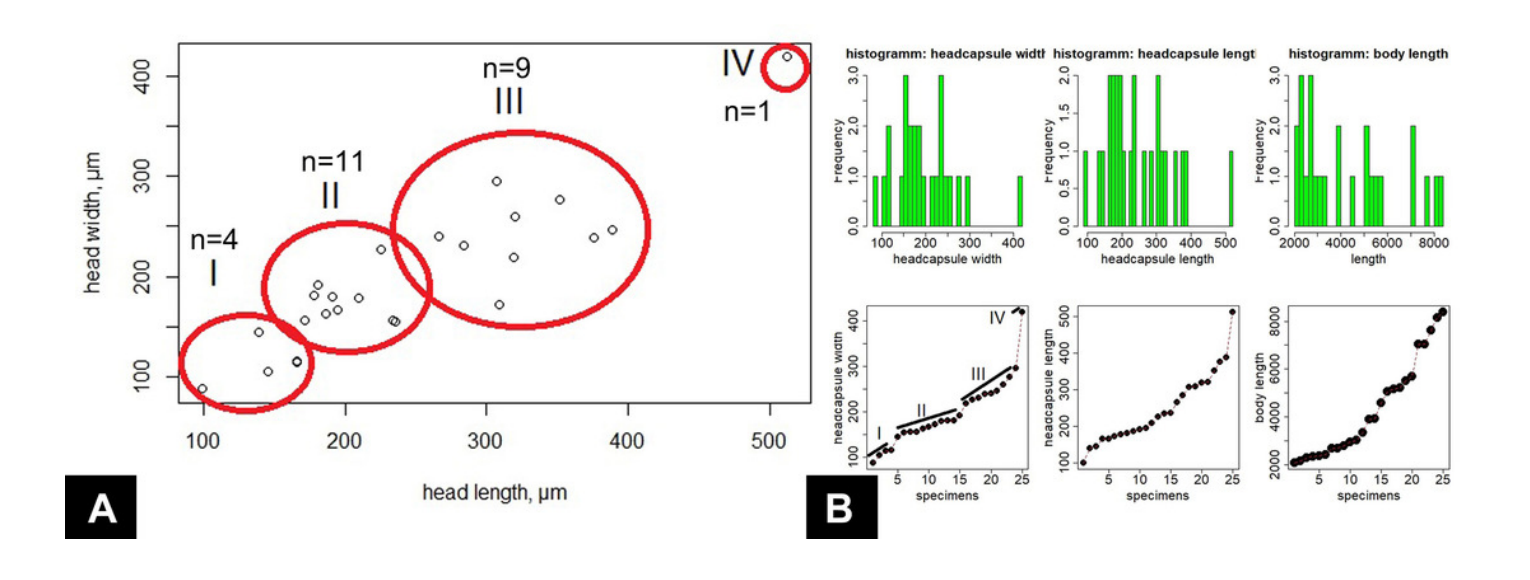
Reconstructed ontogenetic sequence for representatives of *Mycetobia* in the Eocene.





Summary statistics.

(A) biplot of fossil larvae of *Mycetobia* (n=36), head capsule length vs. head capsule width, red circles indicate hypothetical divisions into different larval stages based on the gaps in the data point distribution. I–IV, number of hypothetical larval stages. (B) distribution of the size cohorts within a sample of the fossil larvae of *Mycetobia*; upper-row-left, histogram of the head capsule width distribution (n=26); upper-row-center, histogram of the head capsule length distribution (n=25); upper-row-right, histogram of the body length distribution (n=36); lower-row-left, ranged plot (values ordered in ascending order) of the head capsule width, hypothetical division into different larval stages based on gaps in data point distribution indicated with I–IV as numbers of supposed larval stages; lower-row-centered, ranged plot (values ordered in ascending order) of head capsule length; lower-row-right, ranged plot (values ordered in ascending order) of body length.





Natural logarithm of the mean larval head capsule width and head capsule of fossil larvae of *Mycetobia*, plotted against associated instar number.

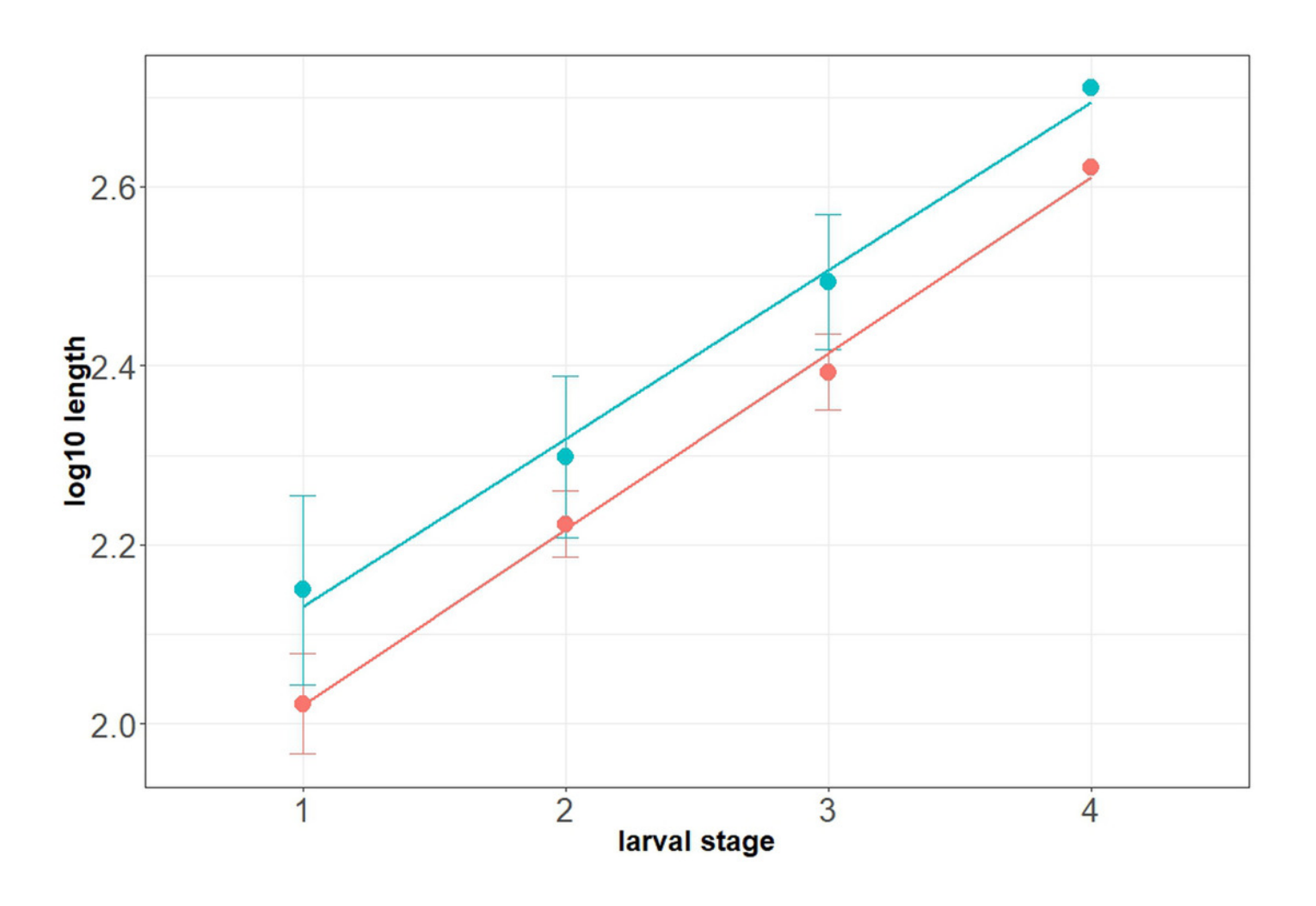




Table 1(on next page)

Table 1. List of material examined



1 Table 1. List of material examined



ID-	<u> </u>				
Number	Taxa	Specimens	Syninclusions	Deposited	Origin
GPIH- Schlee- 0024	Dinobibio hoffeinseorum	1	Acalyptrata	GPIH	Baltic
Dip- 00642	larvae Sylvicola (?)	1	Plant material+ stellate hairs	DEI	Baltic
		male, female,			
PED-4395	Mycetobia connexa	pupal exuvia	partial inclusion of an adult beetle	PED	Baltic
BI-2350	Mycetobia larvae	1	none	GPIH	Bitterfeld
GPIH- 3706 W	Mycetobia larvae	1	Phoridae adult+stellate hairs	GPIH	Baltic
Dip-00639	Mycetobia larvae	1		DEI	Baltic
PED-4965	Mycetobia larvae	1		PED	Baltic
PED-4970	Mycetobia larvae	1		PED	Baltic
PED-5695	Mycetobia larvae	1	Cicadellidae nymph, larva of Coccidoidea, worker ant and non-biting midge female (Diptera: Chironomidae: Tanytarsini)	PED	Baltic
GPIH-L-			Fragment of the Diptera Brachycera female, mites,		
7592	Mycetobia larvae	2	stellate hairs	GPIH	Baltic
Dip-00640	Mycetobia larvae	3	2 males, 1 female Rheosmittia pertenuis	DEI	Baltic
PED-4748 GPIH-	Mycetobia larvae	4		PED	Baltic
Schlee- 0247	Mycetobia larvae	9	"Lepidoptera" (Trichoptera), + fragment of a beetle	GPIH	Baltic
AKBS- 00071	Mycetobia pupa mt 1	1	Lasius schiefferdeckeri+Ctenobethylus geopperti	GPIH	Baltic
GPIH- 1851DN	Mycetobia pupa mt 1	1	2 keratoplatidae males, sciaridae male+ probabbly male of Anisopodidae	GPIH	Baltic
Dip-00641	Mycetobia pupa mt 1	1	Plant material, insect tarsi fragment	DEI	Baltic
GPIH-N- 7095	Mycetobia pupa mt 1	1	Neurothidae larvae, ants 2, Dolichopodidae flies x2, Trichoptera adult, insects i.s. x2	GPIH	Baltic
PED-4998	Mycetobia pupa mt 1	1	spider webs	PED	Baltic
GPIH-L-		1			Batte
7514	Mycetobia pupa mt 2	1	Plant material +stellate hair dult rove beetle (Coleoptera: Staphylinidae) and two	GPIH	Baltic
PED-4866	Mycetobia pupa mt 2	1	adult gall midges (Diptera; Cecidomyiidae)	PED	Baltic
GPIH - 7516	Pachyneuridae larvae	1	stellate hairs	GPIH	Baltic
Dip-00649	Mycetobia larvae	5	Orthocladiinae female	DEI	Baltic
Dip-00650	Mycetobia pupa	1		DEI	Bitterfeld
Dip-00651	Mycetobia pupa	1		DEI	Baltic
Dip-00652	Mycetobia pharrate adult	1		DEI	Baltic
Dip-00653	Mycetobia pupa	1		DEI	Baltic
Dip-00654	Nematocera larvae sp	3		DEI	Baltic
•	Mycetobia pup 2, 2				
Dip-00655	larvae	4	Adult sciaroidea, adult limoniidae	DEI	Baltic
Dip-00656	Mycetobia larvae	3	Ants, Cecidomyiidae,check photo	DEI	Baltic
Dip-00657	Mycetobia pupa mt1	1		DEI	Baltic
Dip-00658	Mycetobia larvae	1		DEI	Baltic
Dip-00659	Mycetobia pupa mt1 Mycetobia pharrate	1		DEI	Baltic
Dip-00660	adult	1		DEI	Baltic
Dip-00661	Mycetobia pupa mt1	1		DEI	Bitterfeld



PeerJ

Dip-00662	Mycetobia pupa mt2	2	ZSM	extant
Dip-00663	Mycetobia pupa mt3	3	ZSM	extant
Dip-00664	Mycetobia pupa mt4	4	CeNak	extant
MB.I.7295	Mycetobia pupa mt1	1	MfNB	Baltic
NA	Mycetobia pallipes Meigen, 1818	>50	ZSM	Ober-Bayern, Fürstenfelderbruck, Roßkastanie, Wundausfluß, Bayern, Germany, 29.5- 4.7.1994, leg. W. Schlacht. Augsburg, Lechau nördl. St. Stephan, Barb-F., Auwald-
NA	Penthetria funebris Meigen, 1804.	>50	ZSM	Ruderal, 440 m, 27.05.1981,Schmidt.
NA	Bibio varipies Meigen, 1830	1	CeNak	NA

2



Table 2(on next page)

Table 2. Morphometry of the fossil Mycetobia larvae from Baltic and Bitterfeld ambers.

Number in the parentheses after accession number indicates number of the Mycetobia syninclusion (if more than one in the same piece of amber). "L"- length, "W"-width



- 1 Table 2. Morphometry of the fossil Mycetobia larvae from Baltic and Bitterfeld ambers. Number
- 2 in the parentheses after accession number indicates number of the Mycetobia syninclusion (if
- 3 more than one in the same piece of amber). "L"- length, "W"-width.

Acession number	L total, μm	head L, μm	head W, μm	larval stage
Dip-00640 (1)	2676.177	145.201	105.129	1
GPIH-0247/8	3346.186	165.624	115.993	1
PED-4748(3)	2283.494	99.005	87.693	1
Dip-00656	2067	166	115	1
Dip-00640 (2)	2151.442	186.238	162.515	2
Dip-00640(3)	2693.354	209.082	178.836	2
Dip-00640 (4)	2405.655	171.311	155.919	2
GPIH-3706 W	2957.863	190.825	180.487	2
BI2350	3909.86	235.719	155.103	2
GPIH-0247(7)	3034.273	195.118	166.481	2
PED-4748(1)	5048.093	309.328	171.883	2
PED-4970	4591.883	233.701	156.178	2
Dip-00656(2)	2784	181	192	2
Dip-00655(1)	2364	139	145	2
Dip-00649(1)	5166	178	181	2
GPIH-0247(9)	3	320.337	259.113	3
PED-4748(2)	5207.932	388.551	246.06	3
PED-4748(4)	10222.51		191.139	3
PED-4965	7027.351	319.331	218.775	3
PED-5695	5503.7	284.294	230.87	3
Dip-00639	7609.245	306.751	295.106	3
Dip-00658	8139	376	239	3
Dip-00656 (1)	5693	266	240	3
Dip-00655(2)	2344	225	227	3
Dip-00649(2)	8385	352	277	3
GPIH-0247(2)	3929.665	512.765	418.808	4
GPIH-0247(1)	5328.197	NA	NA	NA
GPIH-0247(3)	4150.859	NA	NA	NA
GPIH-0247(4)	4898.89	NA	NA	NA
GPIH-0247(5)	1819.851	NA	NA	NA
GPIH-0247(6)	3486.205	NA	NA	NA
GPIH-1-7592(1)	7194.75	NA	NA	NA
GPIH-1-7592(2)	6096.312	NA	NA	NA
GPIH-1-7592(3)	5701.261	NA	NA	NA
GPIH-1-7592(4)	6454.761	NA	NA	NA
GPIH-1-7592(5)	4017.086	NA	NA	NA







Table 3(on next page)

Table 3. Morphometry of the fossil Mycetobia pupae from Baltic and Bitterfeld ambers.

Number in the parentheses after accession number indicates number of the Mycetobia syninclusion (if more than one in the same piece of amber).



- 1 Table 3. Morphometry of the fossil Mycetobia pupae from Baltic and Bitterfeld ambers. Number
- 2 in the parentheses after accession number indicates number of the Mycetobia syninclusion (if
- 3 more than one in the same piece of amber).

Accession number	length, μm	parameter	Morphotype
Dip-00655	1777.074	abdomen	morphotype 1
Dip-00655	1013.289	thorax+head	morphotype 1
Dip-00655	2679.723	total	morphotype 1
Dip-00655	2484.743	abdomen	morphotype 1
Dip-00655	1614.781	thorax+head	morphotype 1
Dip-00655	3842.338	total	morphotype 1
Dip-00652	362.857	thorax+head	morphotype 3
Dip-00652	527.673	abdomen	morphotype 3
Dip-00652	826.356	total	morphotype 3
Dip-00653	2420.659	abdomen	morphotype 1
Dip-00653	1779.554	thorax+head	morphotype 1
Dip-00653	3919.83	total	morphotype 1
GPIH-1851DN	3021.056	abdomen	morphotype 1
GPIH-1851DN	2266.877	thorax+head	morphotype 1
GPIH-1851DN	5059.427	total	morphotype 1
Dip-00641	2340.723	abdomen	morphotype 1
Dip-00641	1624.223	thorax+head	morphotype 1
Dip-00641	3876.262	total	morphotype 1
Dip-00650	320.106	thorax+head	morphotype 3
Dip-00650	645.888	abdomen	morphotype 3
Dip-00650	864.21	total	morphotype 3
Dip-00660	2935.409	abdomen	morphotype 1
Dip-00660	1924.388	thorax+head	morphotype 1
Dip-00660	4238.969	total	morphotype 1
Dip-00661	3647.714	abdomen	morphotype 1
Dip-00661	2220.334	thorax+head	morphotype 1
Dip-00661	5861.01	total	morphotype 1
Dip-00657	2310.204	abdomen	morphotype 1
Dip-00657	1453.298	thorax+head	morphotype 1
Dip-00657	3835.301	total	morphotype 1
GPIH-N-7095.	2154.926	abdomen	morphotype 1
GPIH-N-7095.	1710.244	thorax+head	morphotype 1
GPIH-N-7095.	3761.555	total	morphotype 1
Dip-00659	2466.357	abdomen	morphotype 1
Dip-00659	1697.196	thorax+head	morphotype 1



Dip-00659	3744.385	total	morphotype 1
Dip-00651	2187.597	abdomen	morphotype 1
Dip-00651	1543.324	thorax+head	morphotype 1
Dip-00651	3343.985	total	morphotype 1
AKBS-00071	2490.055	abdomen	morphotype 1
AKBS-00071	1784.352	thorax+head	morphotype 1
AKBS-00071	3630.701	total	morphotype 1
PED-4395	2081.768	abdomen	morphotype 1
PED-4395	1561.697	thorax+head	morphotype 1
PED-4395	3528.726	total	morphotype 1
PED-4866	2596.66	thorax+head	morphotype 2
PED-4866	3041.19	abdomen	morphotype 2
PED-4866	5379.843	total	morphotype 2
PED-4998	2882.949	abdomen	morphotype 1
PED-4998	2174.641	thorax+head	morphotype 1
PED-4998	4811.619	total	morphotype 1
GPIH-L-7514	1826.663	thorax+head	morphotype 2
GPIH-L-7514	2936.171	abdomen	morphotype 2
GPIH-L-7514	4858.746	total	morphotype 2